

Ultrasound

Editors:

Kyle D. Wood, MD

Authors:

Christopher Jaeger, MD; Michael Kurtz, MD, MPH

Last Updated:

Tuesday, February 21, 2023

Keywords

Ultrasound, Radiology, Diagnosis, Imaging

1. Technical Considerations

Ultrasound refers to all sound waves with a frequency above the range of normal hearing, which is about 20 kHz. **Sonography**, which refers simply to the use of ultrasound for medical imaging, typically uses frequencies in the range of 2 to 18 MHz. The sound waves are emitted by an acoustic transducer, which is a component of the ultrasound probe that converts electrical energy into sound energy. Each time the sound waves encounter a material with a different density, an echo is produced, and some portion of the original sound wave returns to the probe. **Hypoechoic tissue reflects less sound than surrounding tissue, while hyperechoic tissue reflects more sound than surrounding tissue. Anechoic tissue does not reflect at all.**

The magnitude of the returning sound wave is related to the **density** of the material from which it reflected, and the **amount of time** that elapsed since emission of the ultrasound wave is related to the depth of the material from which it reflected. If one pulse of ultrasound is sent into tissue, one scan line is produced. A **linear image** is produced by emitting an ultrasound pulse in the same direction, but different starting points. This produces a rectangular image. A **sector image** is produced by emitting an ultrasound pulse from the same starting point, but in different directions. This produces an image shaped like a slice of pie. **B-mode** (or “Brightness” mode) ultrasound refers the process of scanning an entire region and converting the echo strength into the brightness of a single pixel. **Doppler ultrasound** leverages the fact that echoes produced by moving objects have different frequencies than the pulses sent into the body, allowing detection of flow. **Color Doppler** refers to the presentation of velocity information on a B-mode image. **Pulsed wave Doppler** refers to the presentation of velocity information on a timeline. **Duplex** refers to the simultaneous presentation of 2D and pulsed wave Doppler.

1.1 Image Acquisition

Selecting an appropriate transducer is essential to performing a high-quality study. **Linear array**

transducers ([Figure 1](#)) produce the highest resolution images, but the field of view is limited to the size of the probe's footprint. **Sector transducers** ([Figure 2](#)) produce lower resolution images, but can scan a wide region with a small footprint. A **curved array probe** ([Figure 3](#)) is a linear transducer that is curved in order to scan a wider range of tissue, but the main drawback is that the density of scan lines decreases rapidly with increasing distance from the transducer. The optimal frequency of the transducer depends on the depth of the structure being imaged - **higher frequencies provide less penetration, but better resolution**. Therefore, superficial structures are best imaged with high frequency transducers, and deeper structures are best imaged with low frequency transducers. Ultra high-frequency ultrasound refers to use of frequencies in the 15-50 MHz range. The depth of penetration is less than 3 cm but the resolution can be 30 μm as compared to the 200–300 μm of conventional ultrasound using frequencies less than 15 MHz. During image acquisition, common adjustments include gain and depth. **Gain** increases the brightness of the image, while increased **depth** allows deeper structures to be viewed at the expense of reduced scale and frame rate (each line of the image takes longer to acquire).

All probes have markers ([Figure 1](#) and [Figure 2](#)), which correspond to a mark on the screen, often with the company logo. By convention for abdominal ultrasound the marker is oriented cephalad for sagittal images, and to the patient's right side when imaging in the transverse plane. To hold the probe, the thumb is on one side with fingers on the other, and in children it is often useful to place the pinkie against the patient to minimize probe motion relative to the subject. The orientation convention is not held fixed during imaging for intervention.



Figure 1. Linear Array Probe

[Figure 1](#)



Figure 2. Sector Array Probe

Figure 2

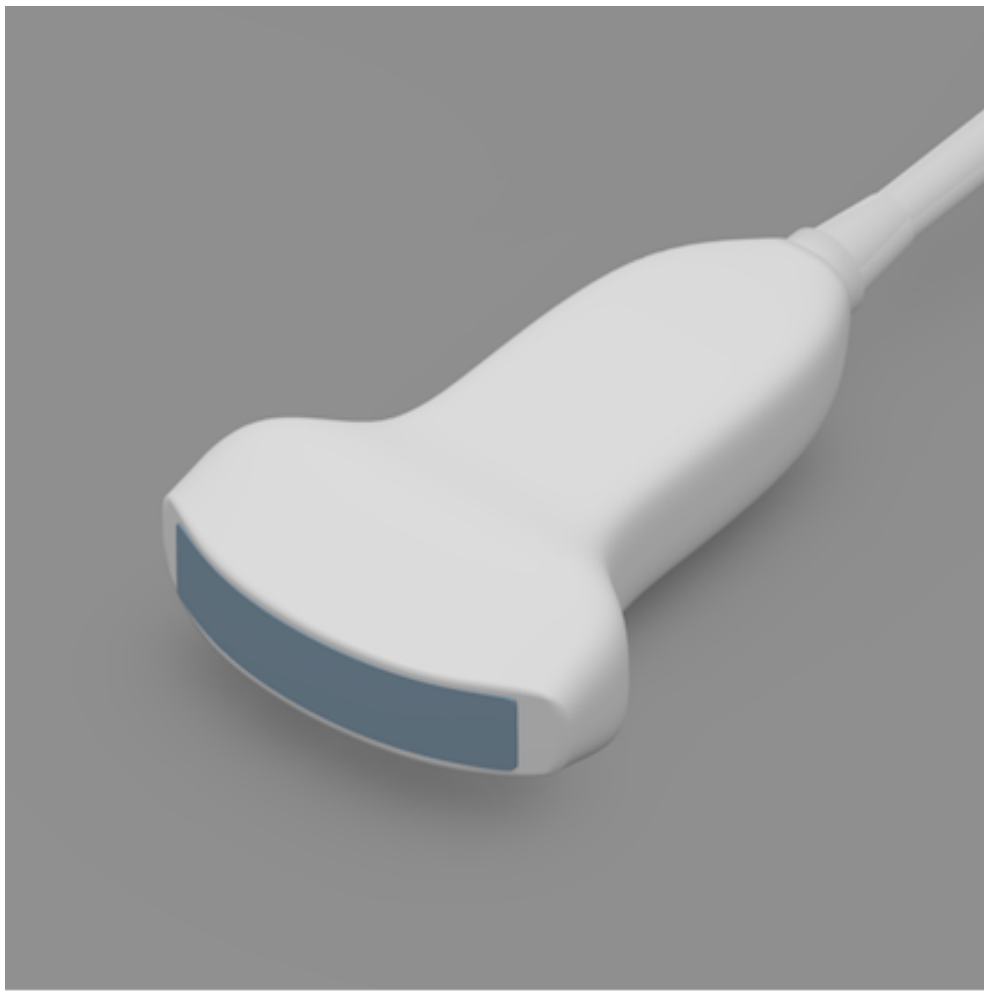


Figure 3. Curved Array Probe

Figure 3

1.2 Artifacts

Knowledge of common artifacts is important in interpreting sonographic images. Artifacts are produced when expectations based on physical principles affecting the sound waves traveling through tissue are not met. Two of these artifacts, enhancement and shadowing, relate to changes in the expected attenuation of the sound wave as it passes through unique tissue types. A well-defined amount of energy is expected to be lost as it passes through tissue. This measurement, based on the physical principles of the sound wave as it travels through tissue, is being continually calculated by the ultrasound processor. When the sound wave passes through a highly hypoechoic structure (e.g., a simple cyst), less loss of the acoustic signal occurs. Therefore, the region behind the structure will receive more sound than the processor expects. As a result, the portion of the image behind a highly hypoechoic structure will appear unusually bright. This artifact is known as increased through transmission or **enhancement (Figure 4)**. The opposite effect, called **shadowing (Figure 5)**, occurs when a structure reflects or absorbs a large amount of energy, and portions of the image behind this structure appear unusually dark. **Anisotropy**, occurs when objects have particularly

smooth boundaries. In these cases, the probe will only receive the reflected sound if the beam strikes the surface at a right angle. Thus, the object will appear bright when oriented at 90 degrees to the ultrasound beam, but dark when the angle is changed.^{1,2} An **edging artifact** (**Figure 6**) occurs when an acoustic wave strikes a curved surface at an angle, known as the critical angle, that allows for propagation of the sound wave along the interface without reflection. This edge artifact is represented on the ultrasound image as a dramatic dark line. It is extremely helpful in demarcating the head of the epididymis from the upper pole of the testis as well as the upper and lower poles of the kidney.

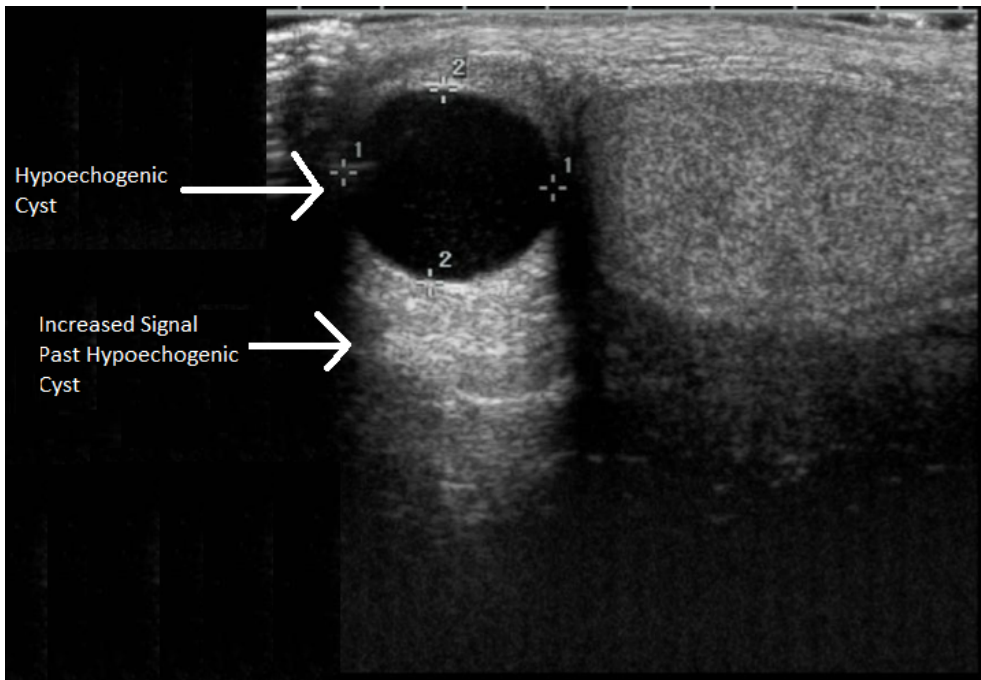


Figure 4. Through Transmission Example - Note signal enhancement in tissue deep to the hypoechoic cyst.

Figure 4

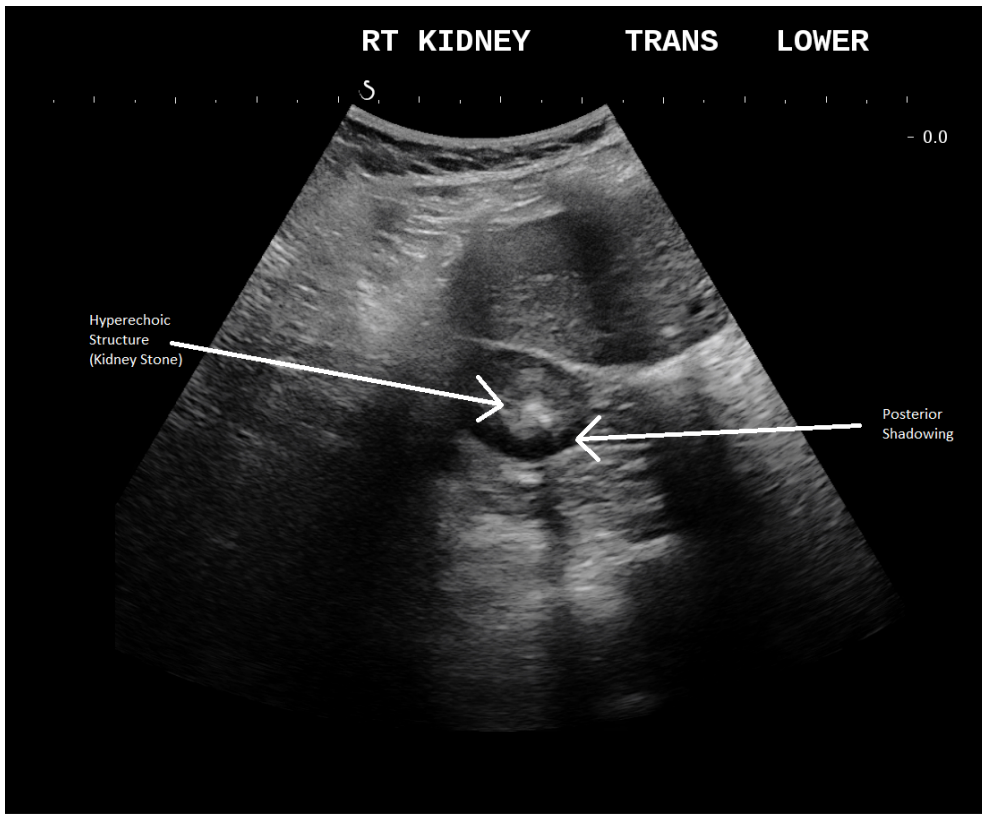


Figure 5. Posterior Shadowing - Hyperechoic structures can prevent signal transduction through them thus resulting in shadowing artifacts posterior to them.

Figure 5

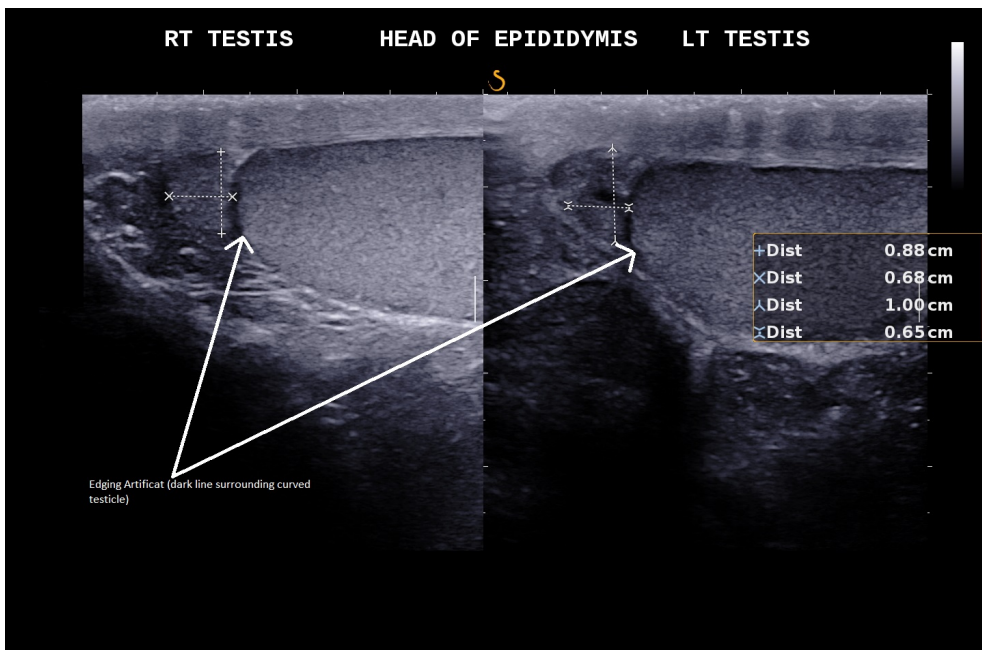


Figure 6. Edge Artifact Curved edge of testicle creates an edge artifact which results in a thick dark line.

Figure 6

2. Ultrasound of Prostate and Seminal Vesicles

Ultrasound of the prostate and seminal vesicles is a useful and highly versatile tool for diagnosis and treatment of a variety of urologic conditions and should be a part of every urologist's armamentarium.

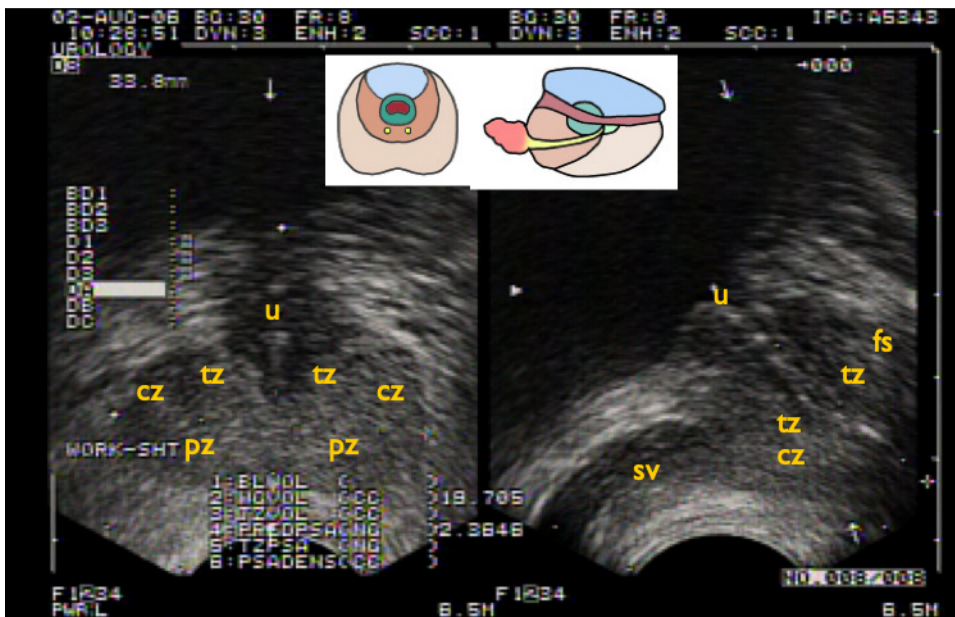
The prostate can be visualized on transabdominal scanning and is routinely documented when evaluating the bladder in the male patient. However, transrectal ultrasound (TRUS) is often preferred due to reduced depth of penetration required and therefore better resolution. TRUS can also be used for transrectal or transperineal biopsies. Measurements are also more precise when obtained trans-rectally.³ Therefore, trans-rectal ultrasound (TRUS) in the left lateral decubitus position is the preferred and widely adopted method for prostate sonography.

2.1. Anatomy of the Prostate

The prostate is in continuity with the bladder base superiorly and the membranous urethra inferiorly. The dorsal venous complex and pubic symphysis lie anterior to the prostate, and the rectum lies posterior. Laterally, the prostate borders the pelvic side wall and the levator ani. Neurovascular bundles are located posterolaterally.

The prostate is classically divided into three zones: **peripheral (PZ), central (CZ) and transition zone (TZ)** (**Figure 7**). In the young adult, the PZ accounts for the majority (> 70%) of the gland. The CZ, which lies anterior to the PZ and behind the proximal urethra, accounts for about 25% of the non-enlarged gland. The TZ are adjacent to the urethra and account for <5 % of the non-enlarged gland. BPH occurs primarily in the TZ and can account for a much larger percentage of prostate volume in patients with advanced BPH. The paired seminal vesicles (SV) appear as hypoechoic structures adjacent to the posterior base of the prostate. The vas deferens travels anterior to the SV and fuses with the ampulla of the SV to form the ejaculatory duct, which travels from the base of the gland through the CZ and empties into the prostatic urethra at the level of the verumontanum.

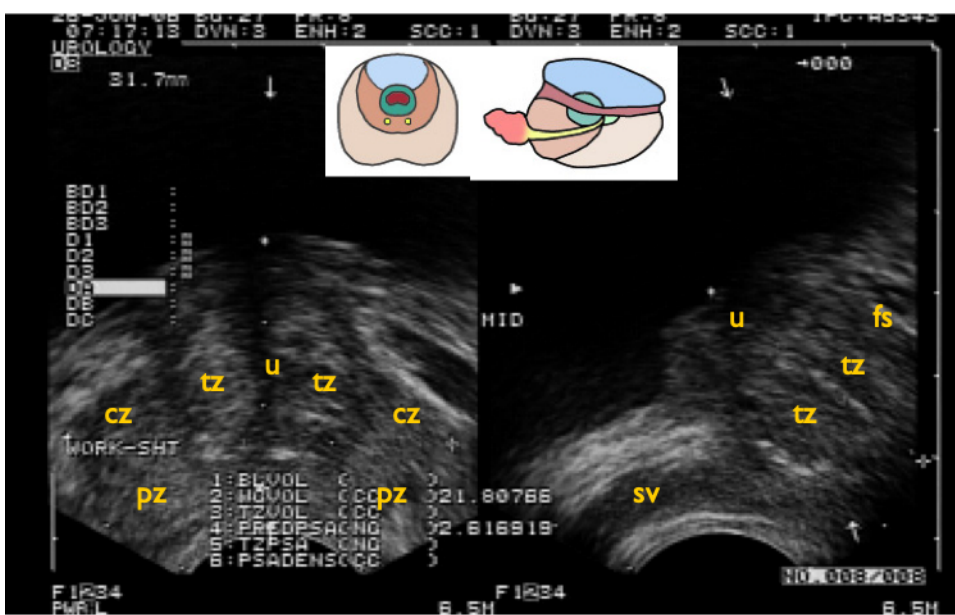
Indications for transrectal prostatic ultrasound are listed on **Table 1**.⁴



mid-transverse

BL: 20 yo male

mid-sagittal



mid-transverse

MS: 60 yo male with LUTS

mid-sagittal

Figure 7. Prostate Zones. CZ - Central Zone, TZ - Transitional Zone, PZ - Peripheral Zone, U - Urethra

Figure 7

Table 1. Indications for Transrectal Ultrasound (TRUS)

Evaluation for elevated PSA

Transrectal and transperineal prostate biopsy

Placement of fiducial markers

Focal cryotherapy

High intensity focused ultrasound treatment of prostate cancer

Evaluation/Aspiration of prostatic abscesses

Evaluation of infertility

Evaluation of prostate size and shape for LUTS/BPH

2.1.1 Equipment and Scanning Technique

As with any sonographic exam, probe selection is essential to a good exam. TRUS can be performed with an end-fire, side-fire, biplaner or triplaner transducers (**Figure 8a, b, c**). Each of these transducers, also called probes, offer advantages and disadvantages. Frequencies of 6-10MHz are appropriate for transrectal imaging, which is often done in conjunction with transrectal or perineal biopsy for prostate cancer. Lower frequency transducers (6 to 8 MHz) have a depth of penetration of 2-8 cm, which is more appropriate for visualization of the transition zone and obtaining accurate volume measurements.



Figure 8a. End-Fire Transducer

Figure 8a



Figure 8b. Biplaner Transducer

Figure 8b



Figure 8c. Triplanar Transducer

Figure 8c

Ultrasound does not propagate through air, so a **coupling medium** (sonographic jelly or lubricant) is used. Typically, a protective condom is placed over the coupling medium and probe. The patient is placed in the **left lateral decubitus position**, with knees bent and hips maximally flexed. The probe is inserted into the rectum slowly to allow for accommodation of the anal sphincter. Gland size is measured in three dimensions, and volume can be estimated by assuming prolate ellipsoid shape

and using the formula (with $\pi/6$ to the hundredths place): **prostate volume = height x width x length x 0.52.**

In a standard diagnostic TRUS study the gland is inspected in the transverse and sagittal planes.⁴ In the transverse plane, advancing the probe cephalad images the prostate base, and moving it caudad images the prostate apex. In the sagittal plane, the probe can be rotated clockwise to image the left side of the prostate or counter-clockwise to image the right side of the prostate. These images can be obtained with a biplaner or triplaner probe without torqueing of the probe.

2.2 Cystic Lesions of the Prostate

Cystic structures of the prostate are common and are clinically significant when they interfere with reproductive function. Congenital cysts can be of Mullerian or Wolffian origin. Mullerian duct cysts appear as midline anechoic lesions that do not communicate with the urethra, whereas an utricle is a special type of Mullerian cyst that communicates with the urethra. This appears sonographically as a midline cystic structure, which is teardrop-shaped in the sagittal plane. It is most commonly associated with hypospadias, is present in 11% of hypospadias patients, and increases in likelihood as hypospadias severity increases. Seminal vesicle and vas deferens cysts are associated with cystic renal disease and renal agenesis. In patients with Eagle Barrett Syndrome, bladder exstrophy or hypogonadism, the prostate may be hypoplastic. Rare diseases such as granulomatous prostatitis, prostatic infarct, and lymphoma appear as hypoechoic lesions.

2.3 Benign Prostatic Hypertrophy (BPH)

BPH is common in men over 40 and is present in the majority of men over the age of 50. **The most common sonographic findings in BPH are asymmetric enlargement, particularly in the transition zone and peri-urethral glands, resulting in deviation of the urethra and elevation of the bladder base.** A median lobe may appear as a mobile mass at the bladder base. Intraprostatic heterogeneity of the inner gland, compression of the peripheral zone (with resulting hyperechogeneity of the peripheral zone), and the presence of adenomas with smooth walls and little internal vascularity are also associated with BPH. TRUS can also aid in assessing prostate size more objectively prior to intervention for LUTS/BPH.⁵

2.4 Findings Associated with Cancer

Traditionally, **hypoechoic lesions** have been associated with prostate cancer (Shinohara et al), though nearly 40% of prostate cancer tumors may be isoechoic. Large contemporary series have failed to demonstrate an increased prostate cancer detection rate in hypoechoic nodules compared to isoechoic nodules.⁶ However, it is currently recommended that all hypoechoic lesions within the PZ should be noted and included in the biopsy material.⁷ The use of sonoelastography has demonstrated sensitivity and specificity of prostate cancer similar to that of MRI. Since most prostate cancers are harder than normal prostate tissue, elastography, which measures the firmness or stiffness of tissue, can be used for evaluation of prostate disease (**Figure 9**).⁸

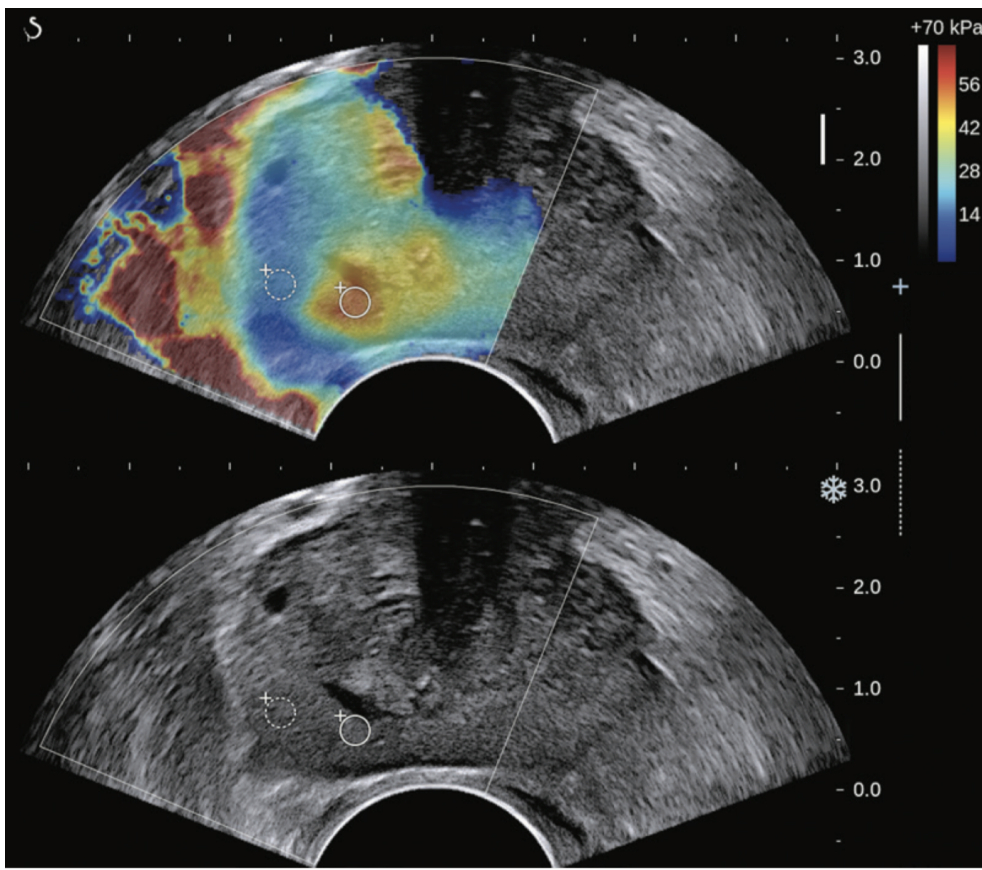


Figure 9. Prostate Elastography. As prostate cancer is harder than normal tissue, elastography, which measures the firmness/stiffness of tissue can be used for evaluation of prostatic disease. Featured here is an elastographic map of the prostate with redder hues indicating denser tissues.

Figure 9

2.5 TRUS-Guided Prostate Biopsy

While screening algorithms continue to evolve, elevated PSA and the presence of palpable nodules on digital rectal exam (DRE) remain the standard indications for TRUS-guided prostate. Transrectal biopsy is a contaminated procedure that carries a low but definite rate of systemic infections (0.1-0.5% in large contemporary studies). A variety of prophylactic regimens have been established to minimize the risk of serious infection, but no standard exists. The American Urological Association Guidelines Best Practice Policy Statement on Urologic Surgery recommends **prophylactic antibiotics prior to transrectal prostate biopsy**, as they have been shown to decrease infectious complications after biopsy.⁹ A single dose of antibiotics is considered equivalent to a 3-day course. Consider multi-drug resistant coverage if patients received systemic antibiotics within 6 months of procedure, underwent international travel, or identify as a healthcare worker. Antimicrobials of choice are fluoroquinolone, 1st/2nd generation Cephalosporin ± Aminoglycoside, or 3rd generation Cephalosporin.⁹ Of note, care must be taken in the administration of quinolones given their black box warning concerning possible tendon damage in elderly populations.

Some practitioners ask patients to self-administer an enema at home prior to the procedure. The potential utility for this is decreased bacterial load in the rectum, which may decrease infectious complications, and lower the amount of feces in the rectum, which may improve probe contact with

the rectal wall, thereby improving image acquisition. There are mixed data regarding infectious complications following topical preparation of the rectum, and the **American Urological Association Best Practice Policy Statement on Urologic Surgery** does not establish a standard for topical preparation of the rectum.

Probe selection for TRUS is described above. The typical biopsy device is a spring-driven 18-Gauge needle core biopsy gun that can be passed through the probe's needle guide.

Positioning for TRUS-guided prostate biopsy is identical to the positioning for TRUS. **Local anesthesia** can be provided by infiltration of local anesthesia around the nerve bundles and, optionally, topical lidocaine per rectum. Though topical lidocaine has little demonstrated efficacy, there is minimal risk. There are good data supporting a local prostate block,^{10,11} which is achieved using 1-2% lidocaine and a long (7-inch, 22-gauge) spinal needle directed through the biopsy channel. Injection can occur at the junction between the seminal vesicle and the base of the prostate, or laterally from the base of the prostate toward the apex. Direct injection into the prostate has some benefit,^{12,13} but there is a risk of systemic side effects from possible intravascular lidocaine injection and absorption.

Most modern ultrasound machines are capable of superimposing a path that corresponds to the needle guide of the TRUS unit. This is helpful in applying local anesthesia as well as obtaining biopsies. When activated, the biopsy gun advances the needle 0.5 cm and samples the subsequent 1.5 cm of tissue. The tip of the needle extends 0.5 cm beyond the sampled area. Therefore, the biopsy may have to be initiated away from the prostatic capsule in order to sample the peripheral zone.

Perineal prostate biopsy under TRUS guidance has recently become more prevalent in an effort to decrease the risk of infection and sepsis following prostate biopsy. While still requiring a transrectal ultrasound probe, the prostate is biopsied through the perineum itself rather than transrectally. In this way, infectious risk is greatly reduced with large series demonstrating a negligible risk of infection.¹⁴ The biopsy itself is performed with the patient in the dorsal lithotomy position, to allow for access to the perineum. Multiple studies have indicated this represents a viable alternative to transrectal biopsy, with effective cancer detection and minimal morbidity. Additionally, authors have demonstrated it is also feasible in an office setting under local anesthesia.¹⁵ A video on free hand TRUS guided biopsy can be viewed [here](#).

TRUS can be combined with MRI for visualization of the prostate using software-based fusion platforms in a procedure known as a MRI/TRUS fusion guided biopsy. The contoured MRI images with identifiable lesions are overlaid on TRUS images. Electromagnetic tracking of the TRUS biopsy probe permits a directed biopsy of the lesions detected on MRI as seen in the [video](#). This strategy can be utilized in combination with systematic biopsies for patients with a clinical suspicion for prostate cancer. Please see **Prostate Cancer Screening, Diagnosis and Risk Stratification** for more details.

TRUS is useful for visualizing the prostate during therapies for prostate cancer and BPH. Additional

uses for TRUS include visualization during brachytherapy seed or fiducial marker placement for prostate cancer.

3. Ultrasound of Scrotum and its Contents

Despite the widespread adoption of more sophisticated imaging techniques in medicine, **ultrasound continues to be the preferred imaging modality for the scrotum**. The superficial structures of the scrotum are well suited for rapid, accurate and inexpensive imaging with ultrasound. Doppler is essential for evaluation of the testicular vasculature. Elastography and contrast techniques have also gained traction to better define disease processes.

3.1 Anatomy of the Scrotum and its Contents

The scrotum, which is composed of skin and underlying fascia, invests and protects the testicles, epididymis and spermatic cords (**Figure 10**). Superficially, the scrotum is composed of skin and Dartos fascia, which condenses in the midline to form the median raphe and divides the scrotum into two functional compartments. Deep to Dartos fascia are external spermatic fascia (continuous with external oblique fascia), cremasteric muscle (continuous with internal oblique muscle and fascia), and the internal spermatic fascia (continuous with transversalis fascia). Deep to this fascia are the testicle, epididymis, and spermatic cord.

The epididymis is located posterolateral to the testis and receives its vascular supply from the spermatic cord, which exits the abdomen through the inguinal canal before entering the scrotum. As the testes descend into the fetal scrotum, peritoneum is brought into the scrotum as well, and this canal becomes the processus vaginalis. The processus vaginalis typically obliterates in utero, leaving peritoneal tissue, or tunica vaginalis, adherent to the testicle and spermatic cord. The inner (visceral) layer of tunica vaginalis covers the testicle and epididymis, and the outer (parietal) layer covers the anterior and lateral parts of the testicle and epididymis. Posteriorly, where the parietal layer of tunica vaginalis is absent, the mesentery inserts into the testicle.

Spermatozoa production occurs in the seminiferous tubules, which enter the mediastinum as the rete testis and then drain into the epididymis. The head of the epididymis abuts the superior testicle while the tail is located near the inferior testicle. The tail of the epididymis drains into the ductus deferens and then the vas deferens, which exits the scrotum with the spermatic cord.

The spermatic cord contains investing fascia (internal, cremasteric and external spermatic fascia) in addition to arteries, veins, nerves, and lymphatics to the testis. The tunica vaginalis is often present in the inferior portions of the cord, but obliterated superiorly. A total of three arteries supply the testis: the testicular artery, which arises from the aorta; the cremasteric (or external spermatic) artery, which arises from the inferior epigastric artery; and the deferential artery, which arises from the hypogastric system and accompanies the vas deferens. They coalesce to enter the testis to become the capsular, centripetal and recurrent rami arteries (**Figure 11**). Venous drainage of the testicle and epididymis occurs via the pampiniform plexus, a network of small veins that unite to become the gonadal vein.¹⁶

Indications for scrotal ultrasound are listed in **Table 2**.⁴

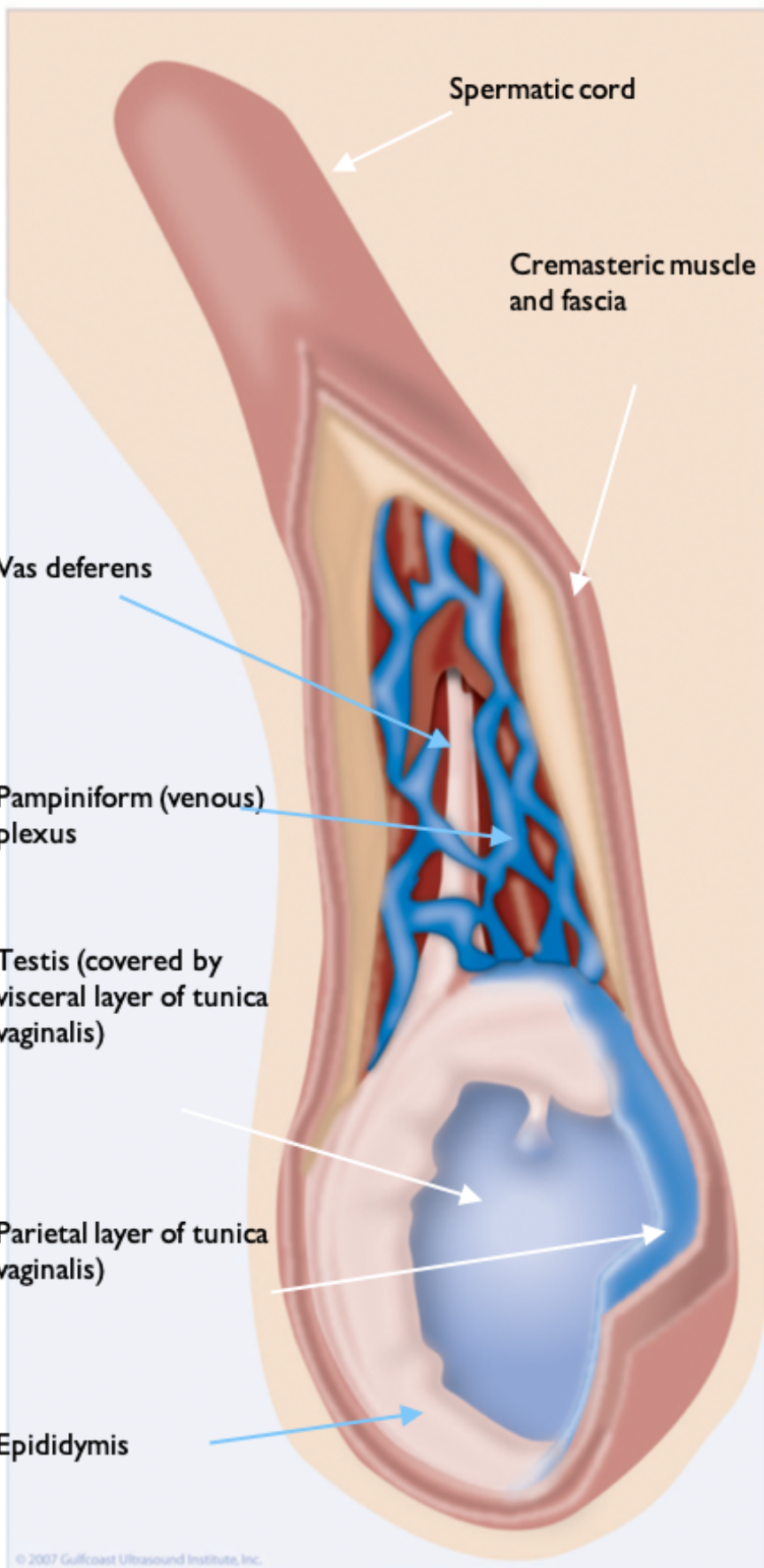


Figure 10. Testis Coverings.

Figure 10

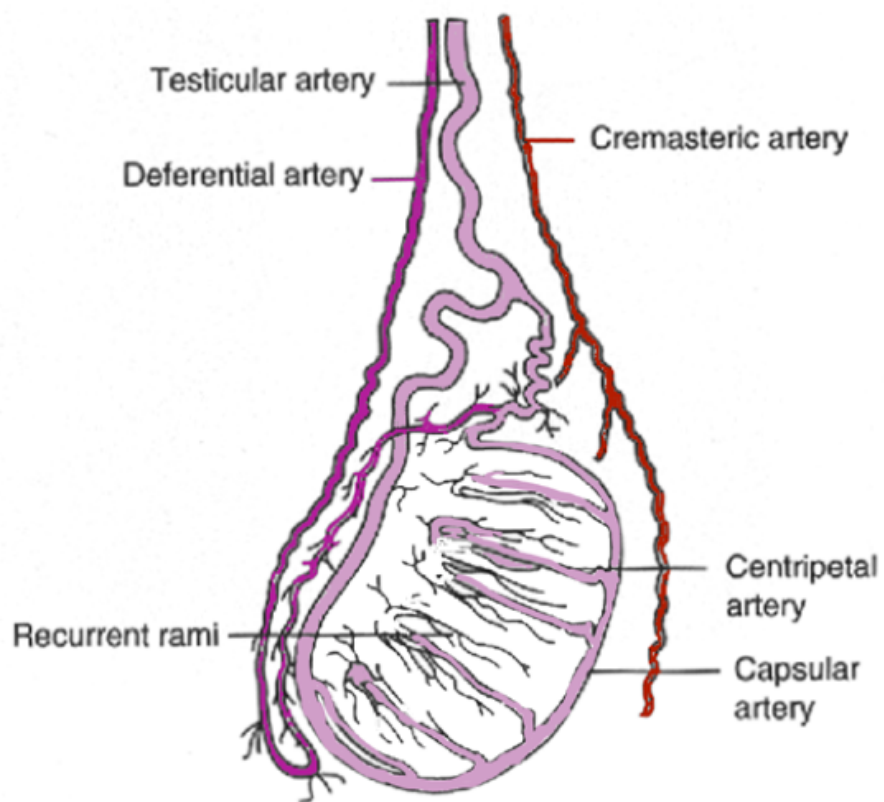


Figure 11 Testicular Blood Supply. The blood supply to the testicle is composed of the testicular, the deferential, and the cremasteric artery.

Figure 11

Table 2. Indications For Scrotal Ultrasound

Palpable scrotal mass

Scrotal mass noted on other modalities

Scrotal trauma

Detection of occult primary tumors in patients with metastatic germ cell tumors

Follow-up after scrotal surgery

Follow-up of patients with prior primary testicular neoplasms, leukemia, or lymphoma

Evaluation for Infertility

Abnormal scrotal sac

3.2 Technique

A quiet, warm room and warm ultrasound gel are important components of a proper scrotal exam. The patient should be in the supine position, with a towel placed under the scrotum to assist with elevation and stabilized by crossing of the ankles. The penis can be held against the anterior abdominal wall by the patient and covered with a towel.

Typically, a **high-frequency (10-18MHz) linear array probe** is used to maximize resolution; probe length should be sufficient to allow longitudinal measurements of the testes. The testis should be imaged in the **sagittal and transverse planes, and simultaneous transverse images of both testicles should be obtained if possible (i.e., “spectacle” view)**. The epididymis, spermatic cord and scrotum should be imaged as well. The testes should be measured in longitudinal and transverse dimensions, and color Doppler should be used to assess flow in the testicles and epididymis.⁴ Color doppler spectacle views are particularly important, and are often the first images acquired, in suspected torsion.

3.3 Normal Appearance

The scrotal wall is typically hyperechoic, and approximately 3 mm in thickness, while the underlying fascia is hypoechoic. The testes are homogenous, of medium echogenicity, and are surrounded by a highly hyperechoic layer corresponding to the tunica albuginea. The **mediastinum testis** appears as a highly reflective linear structure at the posterior-superior aspect of the testicle. The remainder of the testicle is homogenous and of medium echogenicity. Testicular volume can be calculated by the formula: length x width x height x 0.72.¹⁷ Average testicular volume is approximately 1 mL from birth until puberty, when it rapidly reaches normal adult size of approximately 20-30 mL.

3.4 Testicular Cancer

Sonographic appearance of testicular cancer is **variable**. Seminomas tend to appear uniform and hypoechoic, though larger tumors may demonstrate heterogeneity and lobulations (**Figure 12a**). Embryonal tumors tend to be heterogeneous with poorly defined borders that blend into adjacent testicular parenchyma. Choriocarcinomas are often described as a heterogeneous solid mass with areas of hemorrhage, necrosis and calcification. Yolk sac tumors may contain cystic or calcified areas. Teratomas appear as a well-defined complex mass with cystic changes. Calcifications may also be present. Uncommonly, patients with widespread metastatic disease may have areas of calcification or fibrosis in an often atrophic testis, resulting from involuted tumor (**Figure 12b**). Leydig cell tumors are often small, hypoechoic and may have cystic changes, whereas Sertoli cell tumors are often well circumscribed, round and lobulated. Testicular lymphomas appear as discrete hypoechoic lesions with increased Doppler flow. Complete testicular involvement may only be recognized in comparison to the contralateral testicle.

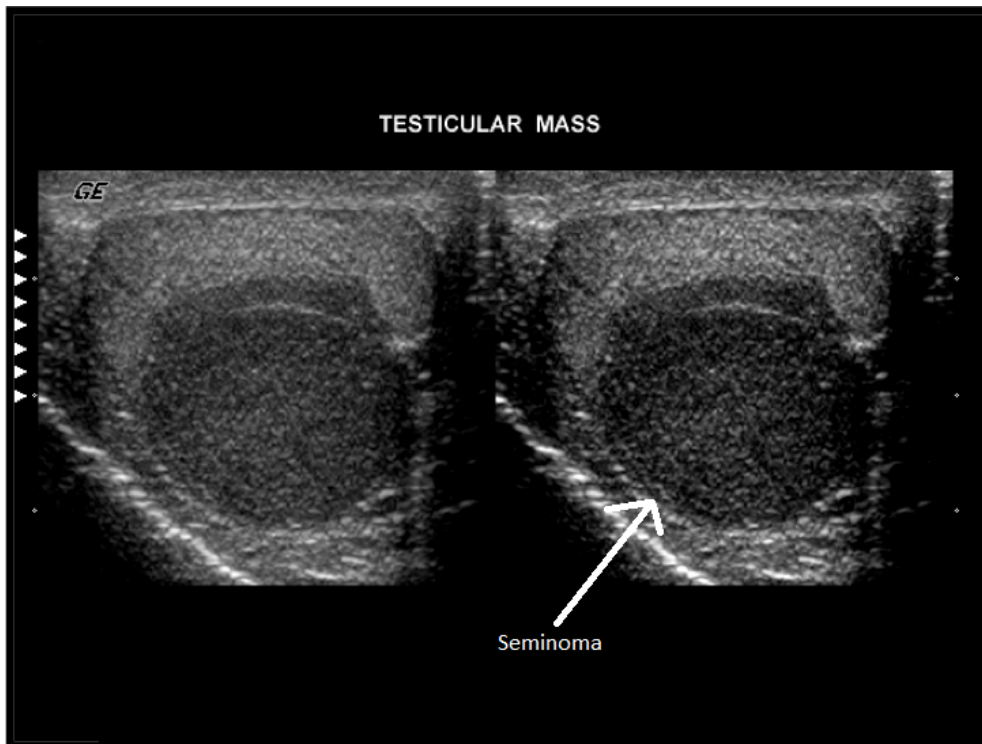


Figure 12a Testicular Seminoma - Seminomas tend to appear uniform and hypoechoic, though larger tumors may demonstrate heterogeneity and lobulations. Pictured here is a round, uniform, hypoechoic testicular mass, compatible with a seminoma.

Figure 12a



Figure 12b Burnt of testicular tumor. In cases of metastatic disease, the testicular tumor may involute/"burnt out" creating a fibrous, calcified lesion in an often atrophic testicle.

Figure 12b. Burnt out testicular tumor. In cases of metastatic

disease, the testicular tumor may involute/"burnt out" creating a fibrous, calcified lesion in an often atrophic testicle.

3.5 Epidermoid Cyst

Thought to arise from monodermal development of a teratoma or squamous metaplasia of surface mesothelium, these lesions have a classic sonographic appearance. **The cysts are well circumscribed and have a highly echogenic border with an avascular, laminated interior (Figure 13), sometimes called "onion skin".** Small cysts with classic radiographic findings and in the context of normal tumor markers may be amenable to enucleation with frozen section pathologic evaluation, though radical orchectomy is an option if concerning features are present.

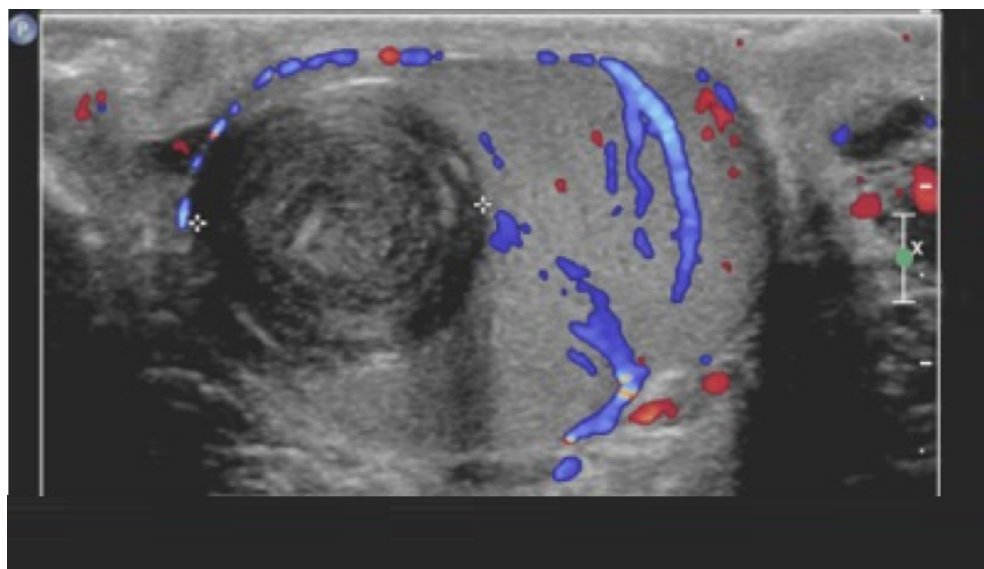


Figure 13 Epidermoid Cyst. An epidermoid cyst, picture here on scrotal ultrasound, appears a well circumscribed, highly echogenic structure with an avascular, laminated interior. Note the lack of blood flow present on the interior of the cyst.

Figure 13

3.6 Epididymitis, Epididymo-Orchitis and Orchitis

The hallmark sonographic feature of epididymo-orchitis and epididymitis is **increased color Doppler flow** (Figure 14). Other common findings are enlargement, decreased reflectivity, and high flow/low resistance waveform on spectral Doppler. A reactive hydrocele may also be present. The infection may involve a portion of the epididymis, the entire epididymis, or may spread to the adjacent testicle. Occasionally, an abscess or septated hydrocele may also be present (Figure 15a). Orchitis without associated epididymitis is rare, but may be caused by the mumps virus. Orchitis is associated with a wide range of sonographic findings, as its appearance evolves over time. Initially, there is edema, and the testicle is diffusely hypoechoic. Over time, the edema consolidates, and the hypoechoic areas become patchy. With more time, there is venous infarction and hemorrhage, leading to a hyperechoic appearance (Figure 15b).

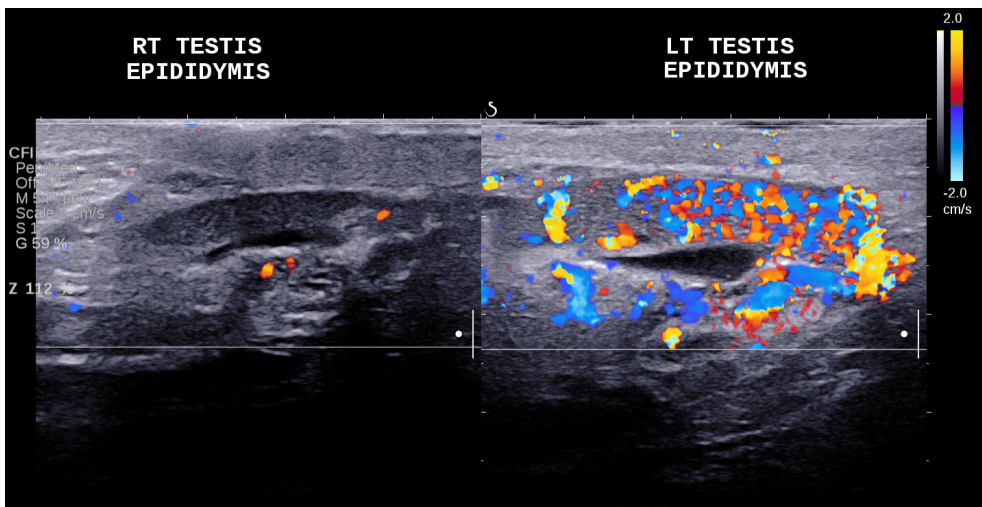


Figure 14 Left Epididymitis. The hallmark sonographic feature of epididymo-orchitis and epididymitis is increased color Doppler flow, see here in the left testis. Other common findings are enlargement, decreased reflectivity, and high flow/low resistance waveform on spectral Doppler.

Figure 14

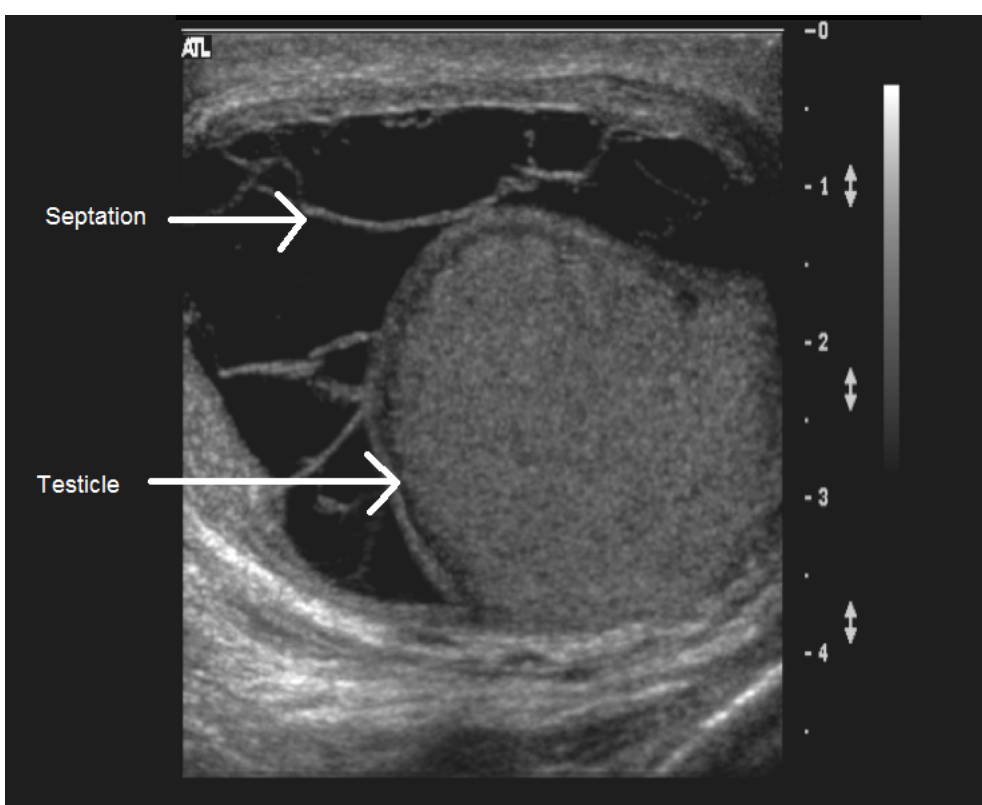


Figure 15a Septated Hydrocele. Hydroceles may occasionally develop thin divisions call septa, resulting in a multi-compartment apperance seen here.

Figure 15a

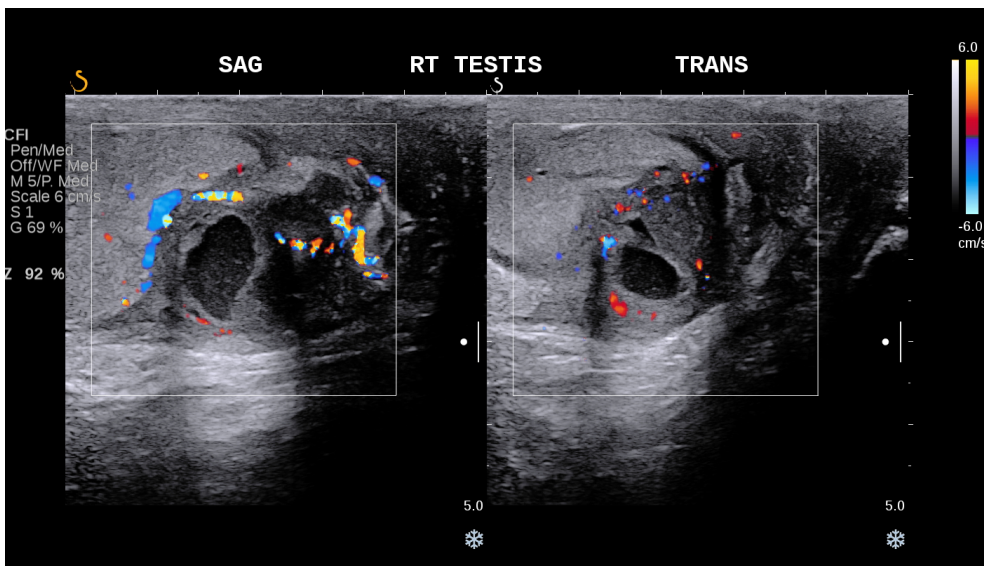


Figure 15b Orchitis with associated abscess formation. Orchitis is associated with a wide range of sonographic findings, as its appearance evolves over time. Initially, there is edema, and the testicle is diffusely hypoechoic. Over time, the edema consolidates, and the hypoechoic areas become patchy. Occasionally, an abscess may develop as pictured here.

Figure 15b

3.7 Epididymal Cysts and Spermatoceles

These entities are cystic structures of the rete testes or epididymal head. A cyst contains serous fluid, whereas debris suggests the presence of spermatozoa and a spermatocele (**Figure 16**). The distinction is not clinically significant, as it does not affect treatment or prognosis. They are generally not painful, but spermatoceles can become large and uncomfortable, in which case they can be removed.

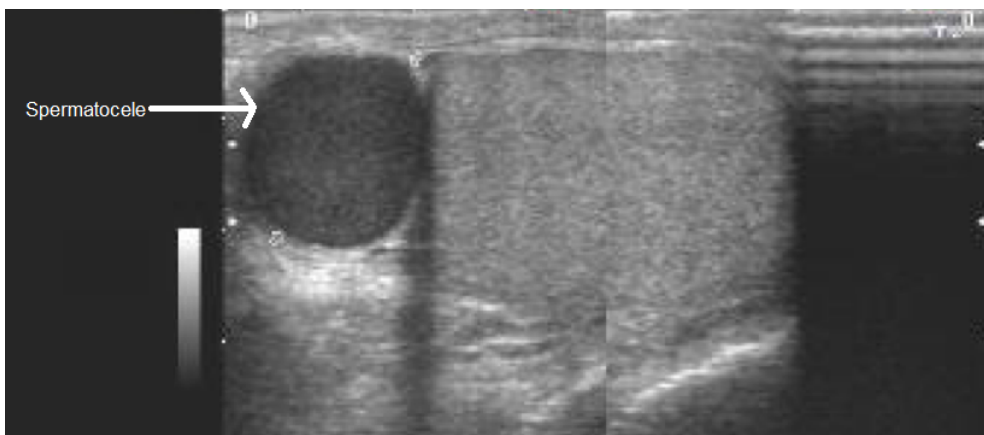


Figure 16 Spermatocele. Spermatoceles are distinguished on ultrasound by a hypoechoic appearance with the presence debris inside it borders. It is picture here (dark grey structure on left) next to the adjacent testicle.

Figure 16

3.8 Adenomatoid Tumor

The most common tumor of the epididymis after an epididymal cyst, they typically present as a painless mass and are benign. Sonographic appearance is non-specific, but they are typically well-defined, isoechoic to the epididymis, oval in shape and can be cystic (**Figure 17**).

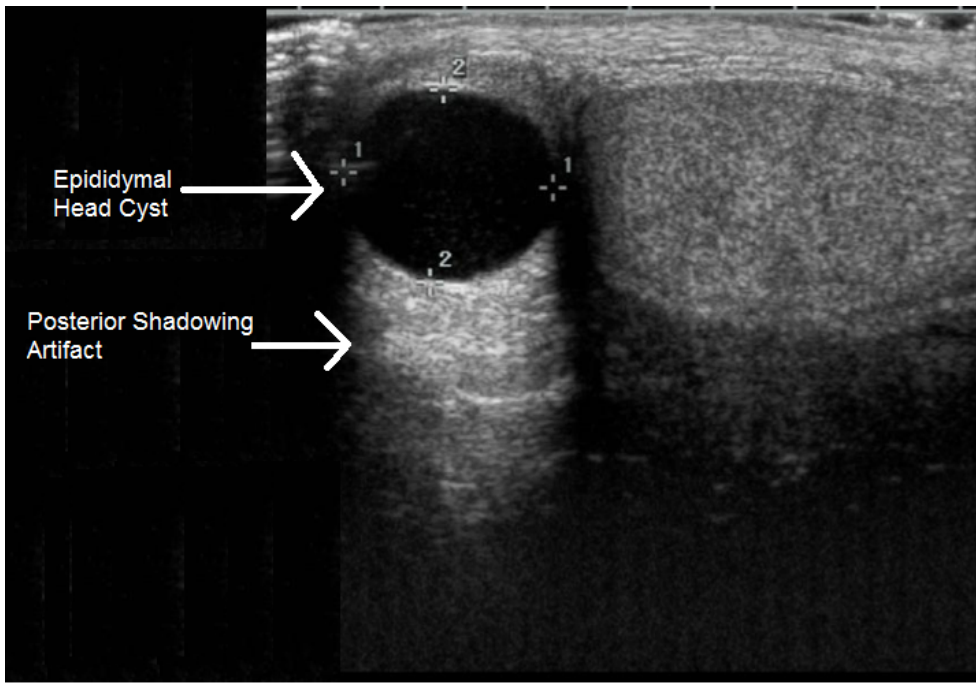


Figure 17 Epididymal Cyst. Cysts appear as well defined, anechocic structures. Note the presence of a posterior shadowing artifact.

Figure 17

3.9 Blunt Trauma

Blunt trauma may result in a variety of injuries to the scrotum and its contents, but the main purpose of the sonographic exam is to detect testicular rupture, or a defect in the tunica albuginea. This is indicated by discontinuity of the tunica albuginea or extravasation of seminiferous tubules outside of the testicle. Complex fluid due to bleeding, a hematocele, may also be present ([Figure 18](#)).¹⁸

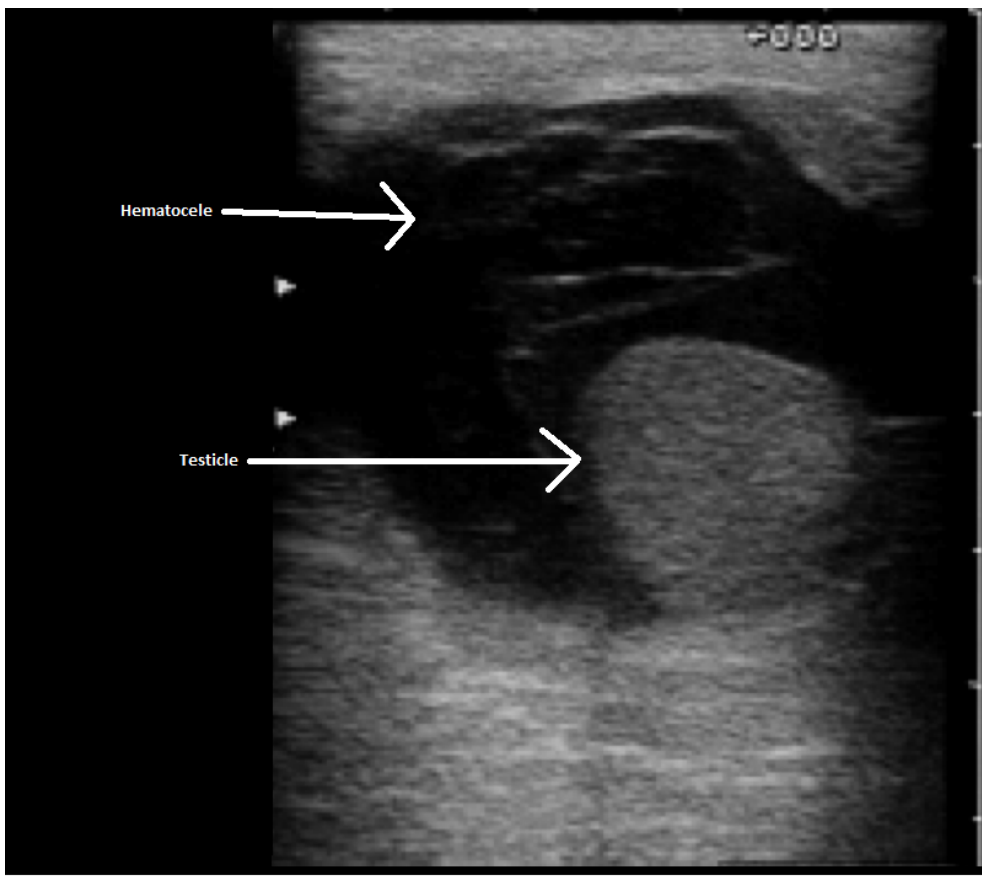


Figure 18 Hematocele. Pictured here is a scrotal ultrasound demonstrating a testicle with a hematocele, appearing as a complex fluid surrounding the testicle.

Figure 18

3.10 Torsion

Torsion of the testicle and spermatic cord typically presents as sudden onset of scrotal pain accompanied by nausea and vomiting and represents a surgical emergency. While clinical diagnosis with surgical confirmation represents the gold standard, scrotal ultrasound represents a highly sensitive test to detect testicular torsion with sensitivity reported from 95-100% with accompanying high specificity.¹⁹ However, in rare cases ultrasound might be misleading demonstrating blood flow when no flow is present and no blood flow when either the ultrasound machine or its settings are inadequate (**Figure 19**). Due to the lower pressure in the venous and lymphatic channels, scrotal edema and venous infarction are the first sonographic signs of testicular torsion. This leads to abnormally enlarged testes with decreased reflectivity, while the tunica albuginea may appear highly reflective. Later, hemorrhage may cause increased reflectivity and heterogeneity. Enlarged, thrombosed pampiniform plexus veins, within the spermatic cord may be visible, and there may be an abrupt change in caliber of the spermatic cord below the point of torsion. Torsion of the testicular or epididymal appendage may also appear with acute onset of scrotal pain, nausea, and vomiting. In these cases, the testicle itself is sonographically normal, and the torsed appendage is typically hyperreflective. Color Doppler may demonstrate an avascular mass separate from the testis with adjacent inflammatory reaction. Note that the epididymis is also edematous in spermatic cord torsion, and an enlarged epididymis viewed in isolation should not prompt a conclusion that epididymitis is

the sole condition present.

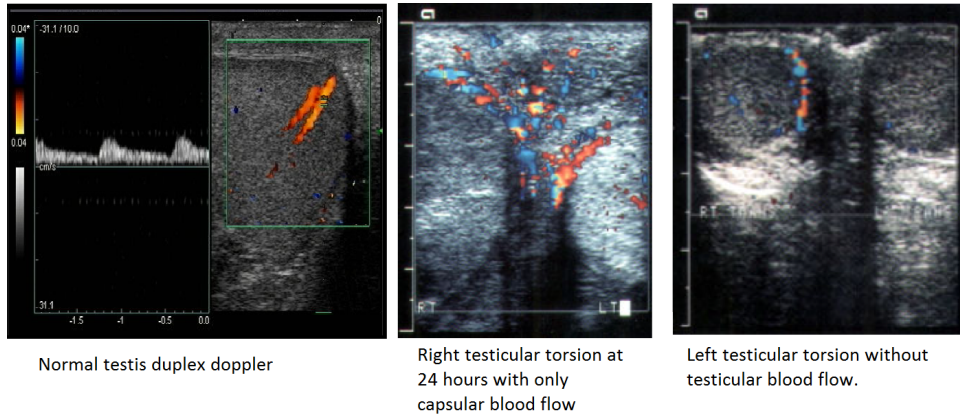


Figure 19 Testicular Torsion. Featured here is a series of doppler flow scrotal ultrasounds depicting normal testicular blood flow and torsion with capsular blood flow and torsion without testicular blood flow. Blood flow appear on color doppler as shades of blue and red depending on directionality from the probe.

Figure 19

3.11 Varicocele

A varicocele is a dilated pampiniform plexus resulting from incompetent valves in the internal spermatic veins (**Figure 20**). Normal veins of the pampiniform plexus measure 0.5-1.5mm; vein diameter > 3 mm visualized either above the testis or posterior to the testis, are considered abnormal. Sonography reveals multiple low reflective tubular structures of varying sizes. These are usually best seen superior and lateral to the testis. Ultrasound should be performed in the supine position. Some sonographers also repeat the study in the standing positions. Valsalva maneuver during the exam will help identify the varicocele and document retrograde filling.

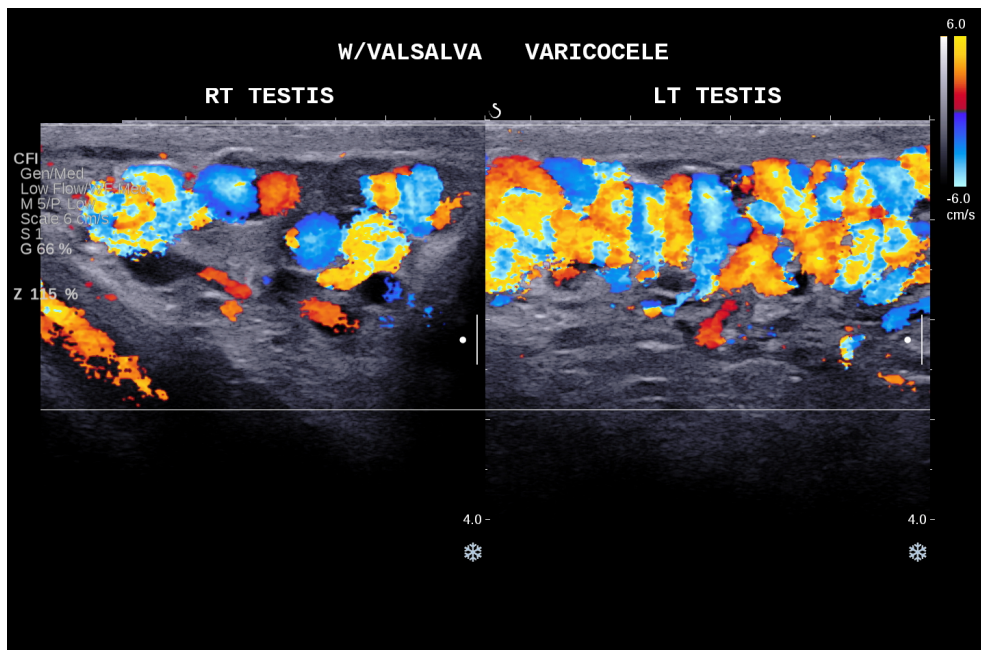


Figure 20 Varicocele. Pictured here on scrotal ultrasound is a varicocele identified by the presence of multiple low reflective tubular structures with internal doppler flow.

Figure 20

4. Penile Ultrasound

Ultrasound is an important and versatile tool for evaluation of the penis and urethra. The superficial nature of these structures enable acquisition of high-resolution images, and the dynamic nature of the exam makes it ideal for assessing distension of structures over time, such as penile vessels during an erection, and compliance of the urethra as it is distended.

4.1 Ultrasound Anatomy

The penis is composed of three cylindrical structures – the paired corpora cavernosa, which are located dorsally, and the ventral corpus spongiosum, which contains the penile urethra (**Figure 21**). The corpus spongiosum expands distally to form the glans penis. Each of these structures is surrounded by a tough fibrous capsule, the tunica albuginea, which exists as two layers dorsolaterally and a single layer that covers both the corpus cavernosum and corpus spongiosum ventrally.

All three structures are enveloped in an additional layer, Buck's fascia, which separates the deep penile structures from the more superficial skin and Dartos fascia. Dorsally, Buck's fascia is continuous with the suspensory ligament of the penis, and Dartos fascia is continuous with Scarpa's fascia of the abdominal wall.

The arterial blood supply to the penis arises from the internal pudendal artery, a branch of the anterior division of the internal iliac artery. The internal pudendal artery divides to form the dorsal penile artery (which supplies the glans penis), the paired cavernosal arteries (which supply the corpora cavernosa) and the bulbar artery (which supplies the corpus spongiosum and urethra) (**Figure 22**). Variations in vascular supply are common, and communication among these end arteries is common.

The corpora cavernosa are of intermediate reflectivity, and the corpus spongiosum is of slightly higher reflectivity. Buck's fascia is readily visualized as a highly reflective line. The cavernosal arteries are located in the center of the corpus cavernosa. The diameter of the cavernosal artery is typically 0.3-0.5 mm in the flaccid state, and greater than 0.7 mm in the normal erect state.

Indications for penile ultrasound are listed in **Table 3**.⁴

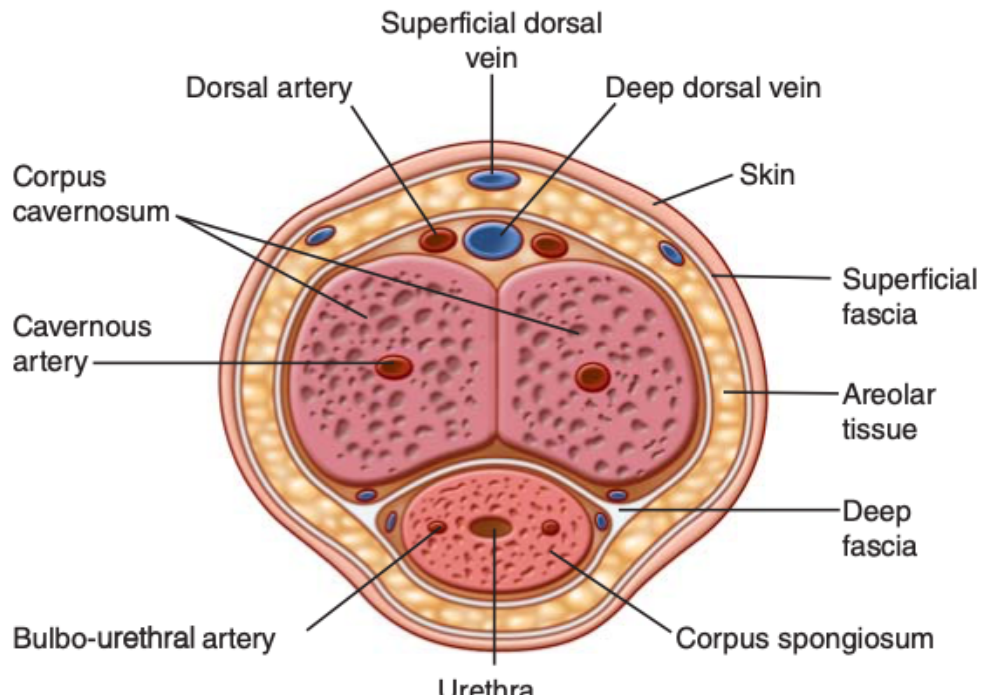


Figure 21 Penile Anatomy (Transverse Section)

Figure 21

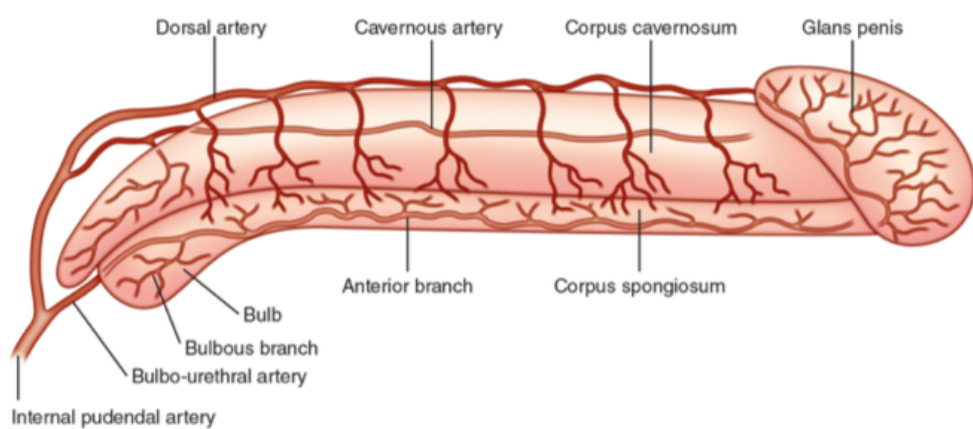


Figure 22 Penile Blood Supply. The blood supply of the penes arises from the internal pudendal artery giving rise to the dorsal artery, the paired cavernosal arteries, and the bulbar artery.

Figure 22

Table 3. Indications for Penile Ultrasound

Erectile dysfunction (ED)

Priapism

Penile trauma/fracture

Dorsal vein thrombosis (DVT)

Penile fibrosis/Peyronie's disease

Penile mass

Penile foreign body

Urethral diverticulum, cyst, or abscess

4.2 Penile Ultrasound

The patient is positioned supine in a quiet, dark room and towels are used to cover the genitals, exposing only the penis. Initial images should include longitudinal and transverse planes from the base of the penis to the glans, with special attention to cavernosal arterial diameter and the presence of calcified plaques within the tunica albuginea.⁴ In pharmaco-stimulation, the area to be injected is cleansed with alcohol, and the injection is performed with a narrow-gauge needle laterally in the corpus cavernosum. A variety of erectogenic medications can be used, and typically consist of alprostadil alone or some combination of alprostadil, phentolamine, and papaverine.

After baseline studies an intracorporeal injection of an erectogenic medication is given and the ultrasound is repeated in 5 minute intervals.⁴ Cavernosal arterial diameter is measured, together with spectral Doppler evaluation of the left and right cavernosal peak systolic velocity (PSV) and end diastolic velocity (EDV) from which the resistive indices are calculated (**Figure 23**). Finally, the presence and location of focal stenosis or cross-communication between cavernosal arteries, which is present in virtually all patients, should be noted.^{20,21}



Figure 23 Penile Cavernosal Artery Duplex. In this penile doppler ultrasound, cavernosal blood flow is classified by end-diastolic velocity (ED), peak-systolic (PS), and resistive index (RI).

Figure 23

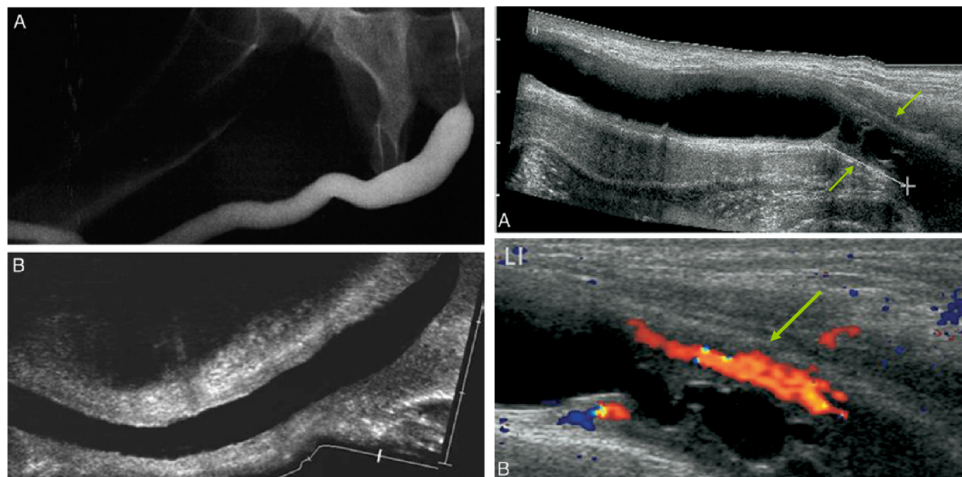
4.3 Urethral Ultrasound

Urethral ultrasound can be performed either in lithotomy or supine with frog-leg positions. Typically, a high-frequency (7.5-12 MHz) linear array transducer is utilized, but a curved probe may be used for the bulbar urethra. Images are obtained in the sagittal plane. Although the urethra can be distended and imaged during physiological voiding, it is typically distended with either saline or sterile

ultrasound gel that is injected through the urethral meatus via a 60 mL catheter-tipped syringe or urethral catheter. Use of 100 mg/5 ml of 2% lidocaine hydrochloride jelly may facilitate image capture and decrease discomfort.²⁰ Typically, injection of several syringes of saline or 15-20 mL lidocaine jelly is necessary to image the entire urethra. Images should be obtained from the distal penile urethra to the proximal bulbar urethra. After the bladder has been filled by several syringes, suprapubic pressure allows for distention proximally, simulating an antegrade study. If a stricture is present, its length, caliber and distance from the external sphincter or other appropriate landmarks should be noted (**Figure 24a**).²²

There has been increasing use of ultrasound contrast agents (UCA) for visualization of urethral pathologies through contrast-enhanced voiding urosonography (ceVUS) or contrast-enhanced retrograde urethrosonography (ceRUG) in the pediatric population for evaluation of male and female lower urinary tracts. For the ceVUS studies, the UCA is administered into the bladder via catheterization until maximal bladder distention. This is then followed by spontaneous voiding or manual suprapubic compression (Crede maneuver) by the technologist. For ceRUG studies, the UCA is administered in the distal urethra. When the urethra is distended with contrast in either technique, it can be visualized with suprapubic, transperineal, and penile transducer positioning.

Figure 24b illustrates examples of a normal urethra and posterior urethral valves on separate ceVUS studies. ceVUS is an imaging technique that continues to evolve but can indeed depict various urethral pathologies.²³



Normal

- A. Radio-urethrography
- B. Sono-urethrography

M Mitterberger et al, J Urol, 177, 992-997, 2007

Urethral Stricture

- A. Sono-urethrography
- B. Color Doppler

Figure 24 Urethral Ultrasound.

Left A. RUG demonstrating no evidence of urethral stricture)

Left B. Urethral Ultrasound with no evidence of stricture.

Right A. Urethral ultrasound demonstrating stricture between green arrows.

Right B. Urethral ultrasound demonstrating tubulent flow through stricture (green arrow) on color doppler.

Figure 24a

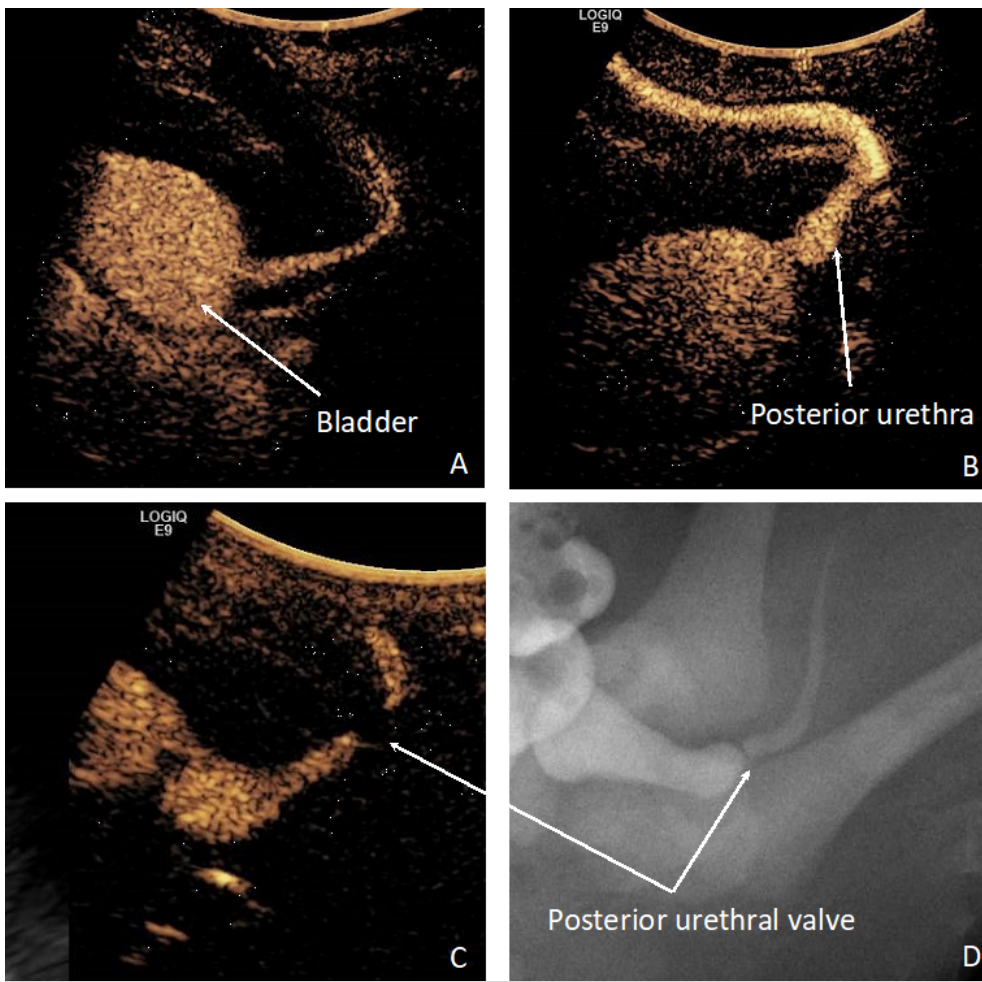


Figure 24b: ceVUS of the Urethra. Images A and B are transperineal, voiding views, performed as part of a ceVUS on a 4 month old boy who had the prenatal diagnosis of hydronephrosis. This reveals normal male urethral anatomy during early initiation of voiding (A) and with a full/strong voiding stream (B). In comparison, the presence of partially obstructing posterior urethral valves is suggested on ceVUS on transperineal voiding views (C) in this 2 day old boy who had the prenatal concern for valves. This is proven on voiding cystourethrogram, re-oriented to match the ceVUS urethral image (D). Images are courtesy of Dr. Carol Barnewolt, pediatric uroradiologist at Boston Children's Hospital.

4.4 Erectile Dysfunction (ED)

Duplex ultrasound of the penis (PDU) with pharmacostimulation can be used as an adjunct to a detailed history and physical examination in the work-up of erectile dysfunction. Arteriogenic erectile dysfunction has been found to correlate directly with other systemic cardiovascular diseases, including both coronary artery disease (CAD) and peripheral vascular disease (PWD), in a number of studies. Therefore, the arteriogenic ED has been found to correlate directly with other systemic cardiovascular diseases, both coronary artery disease (CAD) and peripheral vascular disease (PWD),

in a number of population studies.^{24,25}

In these studies, there was a window of opportunity of two to ten years in which treatment of underlying metabolic abnormalities might be able to prevent future CAD and PVD. Therefore, the results of PDU can improve both the quality as well as possibly the quantity of the patient's life.

Essential questions to answer are whether, during erection, there is sufficient arterial inflow and appropriate venous occlusion. Arterial inflow is represented as the peak systolic velocity (PSV) during erection, and arterial insufficiency is typically defined as **PSV < 25 cm/s**. Inappropriate venous occlusion, or cavernovenous occlusive dysfunction (CVOD), is generally defined as sustained high ($> 5 \text{ cm/s}$) end-diastolic velocity (EDV) in the presence of adequate ($> 25 \text{ cm/s}$) inflow.

Alternatively, a resistive index < 0.75 in the presence of adequate arterial inflow is also consistent with CVOD. Though venous leak is typically diffuse, the presence of a focal site of venous leak should be carefully documented if present, particularly in patients with primary ED.^{26,27}

4.5 Priapism

Doppler ultrasound of the penis is helpful in distinguishing between ischemic and non-ischemic priapism. It is particularly useful in confirming forward flow following a shunting procedure for ischemic priapism, when edema and cavernosal inflammation can mimic a rigid erection. In ischemic priapism, the cavernosal arteries will exhibit minimal EDV, consistent with a high resistance vascular bed. During non-ischemic priapism, the cavernosal artery PSV will be elevated, and will be accompanied by an elevated EDV. The draining veins are often prominent and may exhibit arterialized waveforms. The arterio-sinusoidal fistula will be readily visualized as a focus of high-velocity, turbulent flow (**Figure 25**).²⁸

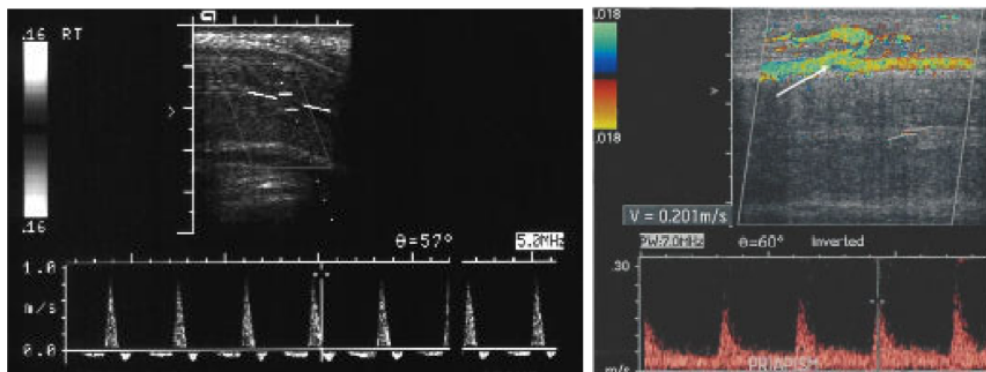


Figure 25 Penile Doppler Penile doppler can be used to distinguish between low flow and high flow priapism. Low flow, when RI > 1.0, represents an emergency necessitating prompt intervention and high flow is represented by RI < 1.0 and does not necessitate prompt intervention.

Figure 25

4.6 Peyronie's Disease

Ultrasound is useful in Peyronie's disease for identifying calcified plaques, which are a contraindication to intralesional therapy and incisional grafting techniques (**Figure 26**). In non-calcified plaques, the presence of increased echogenicity can identify the area of increased

tissue density which can be visualized using elastography in even plaques that are not visible on standard B-mode imaging (**Figure 27**). In patients with Peyronie's disease, the ultrasound is often accompanied by intracavernosal pharmacostimulation in order to document the vascular status of the penis, as poor arterial flow and the presence of venous leak will identify patients who are unlikely to benefit from grafting procedures. This is also an excellent opportunity to visualize the patient's penile deformity, and measurements may be taken at this time with a goniometer or digital device.

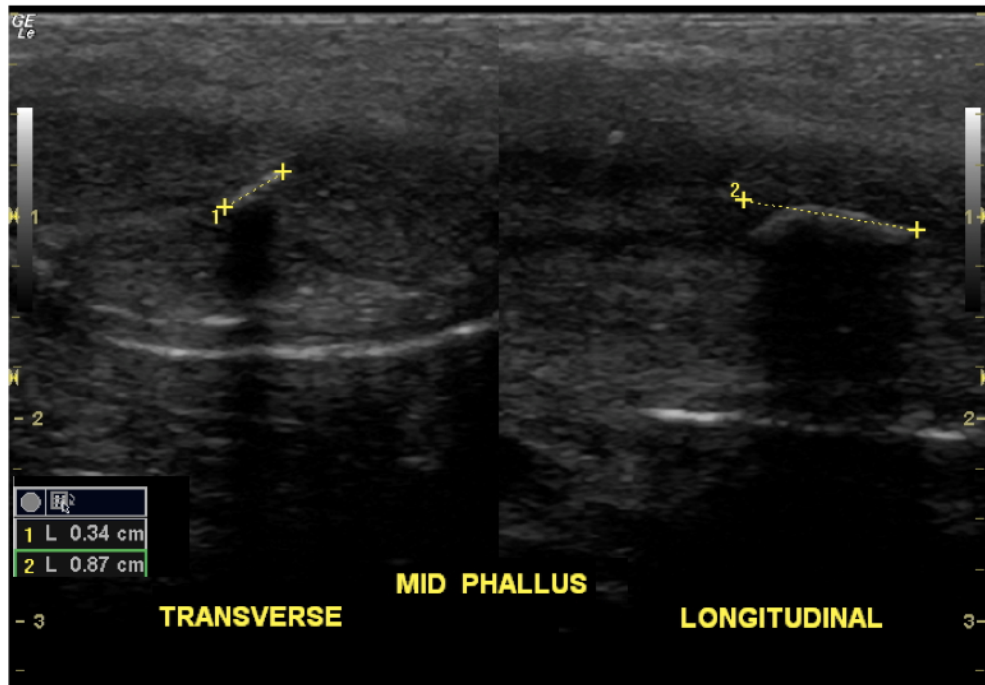


Figure 26 Penile Plaque. Penile ultrasound demonstrating calcified penile plaques (objects 1 and 2 between yellow calipers)

Figure 26

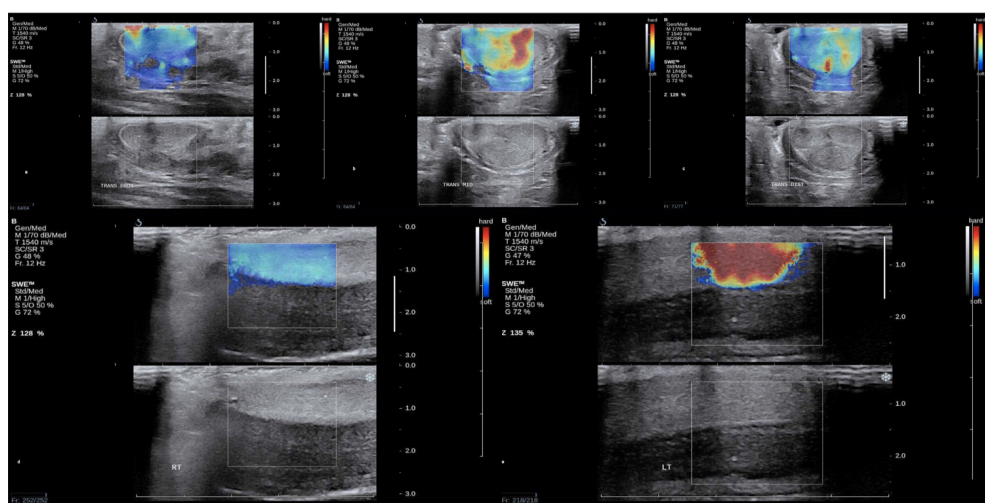


Figure 27 Penile Elastography. Penile ultrasound demonstrating the presence of non-calcified penile plaques in Peyronie's disease through the use of elastography. Penile plaques are identifiable on elastography as areas of increased tissue density, shown in the above figures as red (note right bottom images). These non-calcified plaques are not visible on standard B-mode imaging.

(image reproduced from Richards G, Goldenberg E, Pek H, et al. Penile sonoelastography for the localization of a non-palpable, non-sonographically visualized lesion in a patient with penile curvature from Peyronie's disease. J Sex Med. 2014;11:516–520)

Figure 27

5. Ultrasound of the Kidney

5.1 Anatomic Considerations

Renal ultrasound is an effective tool in the evaluation of numerous urologic conditions. It is highly sensitive and specific in detection of hydronephrosis and can be used selectively in the evaluation of hematuria and urolithiasis. When performed by a properly trained urologist, renal ultrasound allows efficient acquisition of cost-effective and useful information that can be used to guide clinical and surgical decision-making.²⁹

For renal imaging in adults, a **curved array transducer (2.5-6 MHz)** is typically used. Transducers with smaller footprints facilitate image acquisition between the ribs, which is especially helpful for imaging the left kidney, and may provide better surface contact in thin patients.

A thorough understanding of the 3-dimensional orientation of the kidney is critical to effective renal sonography. The lower pole is 15° lateral to the upper pole in the coronal plane. In the transverse coronal plane, the hilum of the kidney is about 30° posteriorly rotated off the true coronal plane. Displacement by the psoas muscle causes the lower pole to be more anterior than the upper pole (**Figure 28a, b, c**). For longitudinal views of the kidney, the orientation of the ultrasound probe should match the long axis of the kidney. This also allows for identification of the true midsagittal plane of the kidney.



Figure 28 Kidney Anatomical Orientation. A thorough understanding of the 3-dimensional orientation of the kidney is critical to effective renal sonography. In the transverse coronal plane, the hilum of the kidney is about 30° posteriorly rotated off the true coronal plane. The lower pole is 15° lateral to the upper pole in the coronal plane. Displacement by the psoas muscle causes the lower pole to be more anterior than the upper pole.

Figure 28a, b, c

Ultrasound of the right kidney is typically performed with the patient in the supine position. The transducer is placed in the mid-clavicular line at the level of the costal margin. Bowel gas in the transverse colon will often be encountered initially. The transducer is swept laterally using the liver as an acoustic window to image the upper pole of the right kidney. The homogenous composition of the liver offers excellent transmission of the sound waves with minimal distortion. As the transducer is moved more laterally, the kidney can be more completely imaged without interference from bowel gas. An attempt should be made to find the true midsagittal plane of the right kidney. This serves as an anatomic landmark from which the remainder of the complete scan can be performed. The midsagittal plane of the kidney is characterized by the longest measurable sagittal axis of the kidney. The renal parenchyma is discontinuous medially in the mid-sagittal plane at the level of the entry and exit of the renal vessels and the exit of the renal pelvis from the renal sinus (**Figure 29**). In children,

this is the view in which the anterior-posterior diameter of the kidney is correctly measured.³⁰

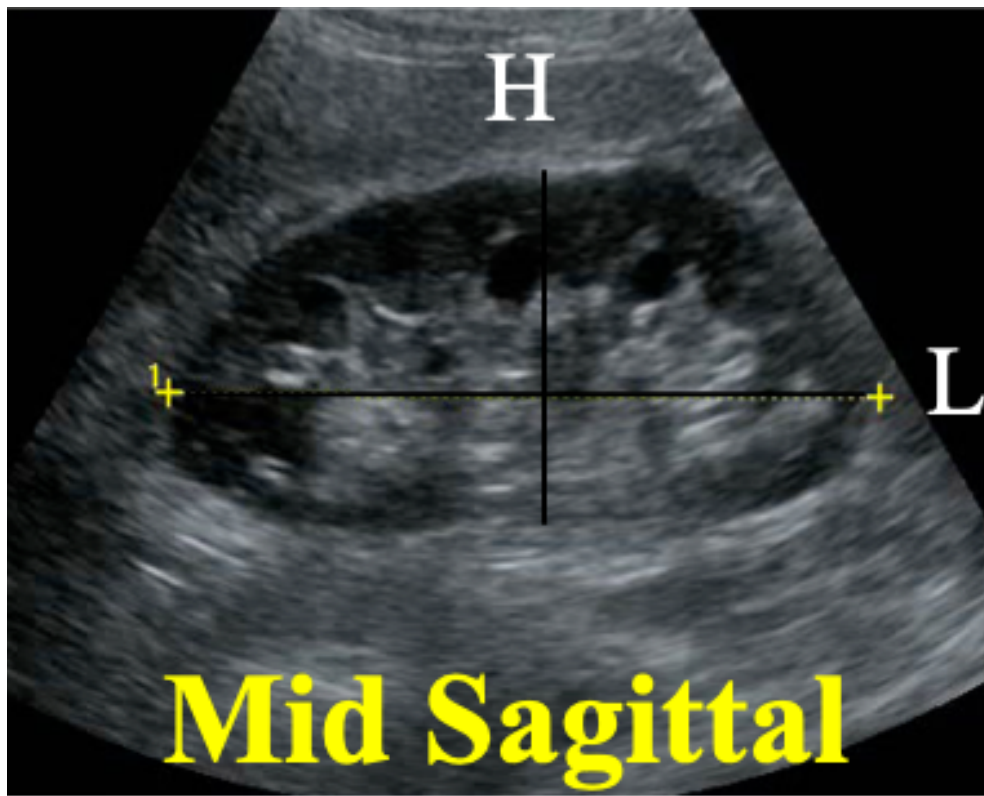


Figure 29 Renal Mid-Sagittal View. The midsagittal plane of the kidney is characterized by the longest measurable sagittal axis of the kidney. The renal parenchyma is discontinuous medially in the mid-sagittal plane at the level of the entry and exit of the renal vessels and the exit of the renal pelvis from the renal sinus

Figure 29

Once the midsagittal plan is localized, the kidney should be scanned anteriorly and posteriorly until the entirety of the renal parenchyma has been evaluated. The upper pole and mid kidney can usually be viewed through the liver window. The lower pole frequently has to be viewed directly via a more lateral or posterior location. From the midsagittal plane, rotating the transducer 90° counterclockwise will image the midtransverse plane of the kidney. This is characterized by a horseshoe-shaped renal parenchyma discontinuous on the medial aspect at the level of the renal sinus. It is often possible to see the renal vein sonographically in this view. The renal artery is more difficult to visualize. Once the mid-transverse plane has been identified, the kidney is scanned through the upper pole and through the lower pole. This evaluation can be accomplished by moving the probe cephalad and caudad and by having the patient take a deep inspiration to bring the upper pole of the kidney into view. Once the kidney has been completely evaluated in both planes, attention is turned to identifying and documenting normal and abnormal findings.³¹

Ultrasound of the left kidney is typically performed with the patient in the right lateral decubitus

position, as bowel contents typically interfere with an anterior approach. However, this approach will often result in a greater attenuation and scattering by flank and back musculature when compared to supine images of the right kidney. The patient's left arm is placed over the head in order to open the intercostal spaces and create a wider imaging window. The transducer is placed at the mid axillary or posterior axillary line. The spleen is frequently seen anterior and superior to the left kidney, but is not usually well positioned to use as an acoustic window. The true midsagittal view of the left kidney is then located. This will be the plane of the longest sagittal length of the kidney. The renal capsule will appear discontinuous at the mid kidney medially at the site of the renal hilum. In the coronal view, cortical tissue is seen as a continuous ring around the hyperechoic pelvic sinus fat except at the renal hilum (**Figure 30**). Once the anterior and posterior surfaces have been fully imaged in the sagittal plane, the probe is rotated 90° to image in the axial plane. The left kidney assumes a horseshoe shape with the discontinuity of the parenchyma orientated medially at the location of the renal sinus. The upper lower poles of the left kidney are imaged completely by moving the probe cephalad and caudad and with targeted breathing by the patient as necessary. A deep inspiration and expiration will move the kidney several centimeters. Once the kidney has been completely evaluated in both planes, attention is turned to identifying and documenting normal and abnormal findings.⁴

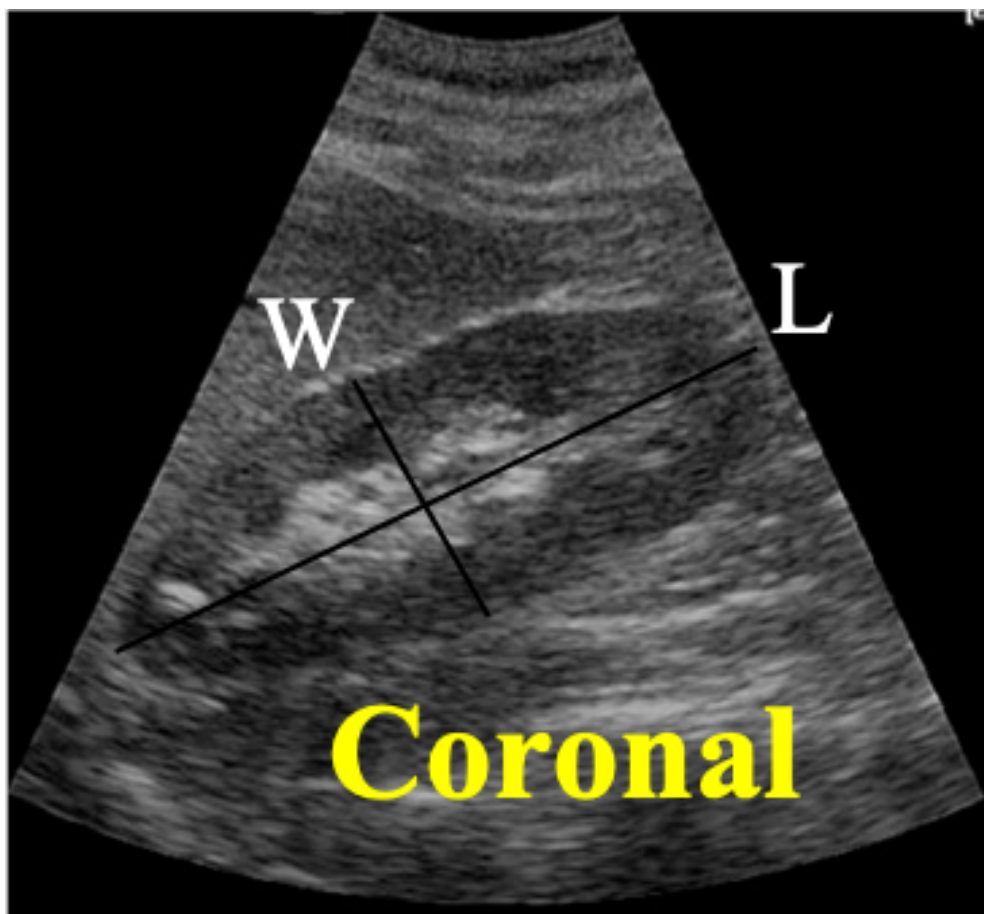


Figure 30 Coronal View of Kidney. In the coronal view, cortical tissue is seen as a continuous ring around the hyperechoic pelvic sinus fat except at the renal hilum.

Figure 30

Renal contours should be smooth and of an oval reniform shape, losing fetal lobation in infancy and early childhood. Any deviation from a smooth uniform contour should be noted and a representative image saved. All surfaces of the kidney should be scanned from top to bottom and from anterior to posterior. The kidney measurements should be recorded. The transverse view of the mid kidney should be measured, and the image saved. An image of the midline longitudinal length should be measured, and the image saved. Care should be taken to ensure that the true midline longitudinal view of the kidney is obtained for accurate measurement of length. Normal adult kidneys measure 10-12 cm longitudinally, 5-7 cm transversely, and 3 cm in the anteroposterior dimension. The right and left kidneys should be of similar size. Any size discrepancy should be noted in the report. A discrepancy in the long axis of over 1.5 cm is considered abnormal.

Renal cortical thickness should be relatively uniform throughout the kidney. Any bulges or indentations in the cortex should be noted on the report and captured as an image. The cortical thickness is measured from the renal capsule to the base of the triangular medullary pyramids. The parenchymal thickness is measured from the renal capsule to the edge of the renal sinus. In adults, the medullary pyramids are often indistinct on ultrasound imaging, and thus measuring an accurate cortical thickness can be difficult. Normal renal parenchymal thickness is 1.5 cm. A renal parenchymal thickness under 1 cm is considered to be abnormal.³¹

The normal adult renal cortex should appear hypoechoic or iso-echoic relative to the normal liver or normal spleen. The normal renal cortex should appear homogenous in echogenicity. The medullary pyramids should be hypoechoic compared to the renal cortex. Due to the presence of vascular structures, sinus fat and collecting system, the renal sinus is highly echogenic compared to normal renal cortex.

The indications for renal ultrasound are lengthy and diverse, and are listed in **Table 4**. As a non-invasive, inexpensive test without radiation exposure, it should be utilized whenever possible before cross-sectional imaging such as CT or MRI. **Moreover, Doppler technology can evaluate the vascularity of renal masses.**

Recently, Chi et al. demonstrated that the addition of microbubble US contrast agents to conventional US has expanded the repertoire of US.³² The dynamic real-time assessment of the vascularity in visceral organs, with spatial and contrast resolution, can be used to assess antegrade ureteral patency in patients with nephrostomy tubes. It also has potential advantages over fluoroscopy regarding patient safety (including radiation exposure) and convenience. Larger scale studies need to be done to evaluate diagnostic accuracy of this technique relative to current standard of care.

Indications for renal ultrasound are as listed in **Table 4**.⁴

Table 4. Indications for Renal Ultrasound

Flank and/or back pain with concern for urolithiasis or abscess
Acute renal injury/failure with concern for obstruction
Gross Hematuria
Abdominal trauma
Evaluation of microscopic hematuria in low-risk patients who elect to undergo testing
Evaluation of microscopic hematuria in intermediate-risk patients
Evaluation of microscopic hematuria in high-risk patients with contraindications to CT and MRI
Active surveillance for renal mass
Surveillance for known renal and ureteral stones
Pre- and post-transplant renal evaluation
Further evaluation of abnormal findings of the kidney on other imaging studies
Follow-up after initial treatment of a low risk renal malignancy
Pediatric indications include antenatal and postnatal urinary tract dilation (UTD) evaluation, workup of congenital anomalies such as duplex kidney or UPJ obstruction, and febrile UTI
Planning and guidance for interventional procedures including percutaneous nephrostomy tube placement, renal biopsy, renal cyst aspiration/sclerosis, and renal mass ablation
Intraoperative renal parenchymal and vascular imaging for ablation or resection of tissue

5.2 Hydronephrosis

Renal ultrasound is highly sensitive for the detection of hydronephrosis and is a useful tool for monitoring collecting system distention over time, such as after ureteropelvic junction repair, ureteral reimplantation, or treatment of ureteral stricture.

5.3 Parapelvic Cysts

Parapelvic cysts are anechoic structures of varying size adjacent to or within the renal sinus. Occasionally, the cyst penetrates deeply into the renal sinus, mimicking dilated calyces and suggesting hydronephrosis. In these cases, it is helpful to evaluate the location of the cyst in relation to the medullary pyramid. In hydronephrosis, the long axis of the hypoechoic structure tends to line up pointing towards the renal papilla and pyramid, whereas parapelvic cysts tend to have their long axis pointing in between pyramids.

5.4 Renal Cysts

Renal cysts are well characterized with ultrasound. A simple cyst is defined by three sonographic findings: (1) anechoic contents; (2) walls are thin, smooth, and well defined; and (3) posterior acoustic enhancement beyond the cyst. The **Bosniak classification** was developed for characterizing renal cysts on CT but is often extended to describing cysts seen on ultrasound examinations.³³

5.5 Renal Scars

Parenchymal scarring appears as a sharp depression in the outline of the kidney. Scars are always typically over renal pyramids, often are polar affecting compound calyces, and the cortex is dramatically thin or absent in the region of the scar. Nuclear imaging is a more sensitive modality.

5.6 Renal Masses

Though not as sensitive as CT or MRI at detecting and characterizing renal masses, renal ultrasound can be used to monitor renal masses over time. It is particularly helpful for monitoring growth rate while limiting exposure to ionizing radiation especially for patients with hereditary renal masses. Of note, angiomyolipomas may have internal hyperechoic findings due to the fat content within these commonly benign renal masses. Further characterization with abdominal CT or MRI can further confirm likelihood of this diagnosis.

Renal ultrasound can also be used intraoperatively during a partial nephrectomy for identification of renal masses. Doppler modes and contrast-enhanced ultrasonography (CE-US) via microbubble technology can assist in selective ischemia for improved visualization of tumors.³⁴ Both options come with laparoscopic ultrasound probes such as the one pictured below (see **Figure 31**). Ultrasound images are projected onto the console screen without having to leave to see images on an external screen.

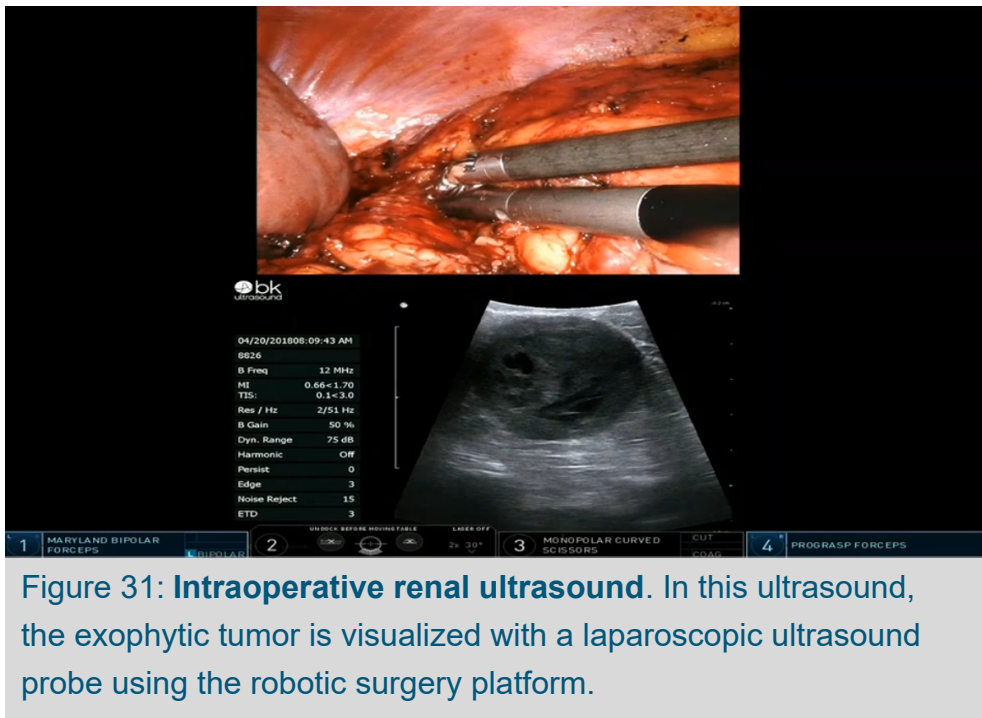


Figure 31: Intraoperative renal ultrasound. In this ultrasound, the exophytic tumor is visualized with a laparoscopic ultrasound probe using the robotic surgery platform.

5.7 Urolithiasis

Ultrasound can be a valuable tool in evaluating urolithiasis especially in the hands of well-trained sonographers. The use of artifacts including posterior shadowing and the twinkle artifact (**Figure 32**) together with elastography are useful techniques for evaluating small and large calculi. Renal ultrasound has limited sensitivity for stones less than 2-3 mm in size and is less sensitive and specific than CT for detecting calculous presence and location. Despite its limitations, it remains the study of choice for pregnant patients and pediatric patients with renal colic. In one study of pediatric patients, it was found that renal ultrasound has a 76% sensitivity and 100% specificity for detecting stones compared to CT.³⁵

Renal ultrasound can also be used for percutaneous access to the collecting system within the kidney for nephrostomy tube placement or percutaneous nephrolithotomy (PCNL). Comparative studies evaluating ultrasound-guided access with fluoroscopic access have mixed results; however, ultrasound-guided access is feasible and does not emit radiation. More details can be found at the AUA Core Curriculum **Urolithiasis** section.

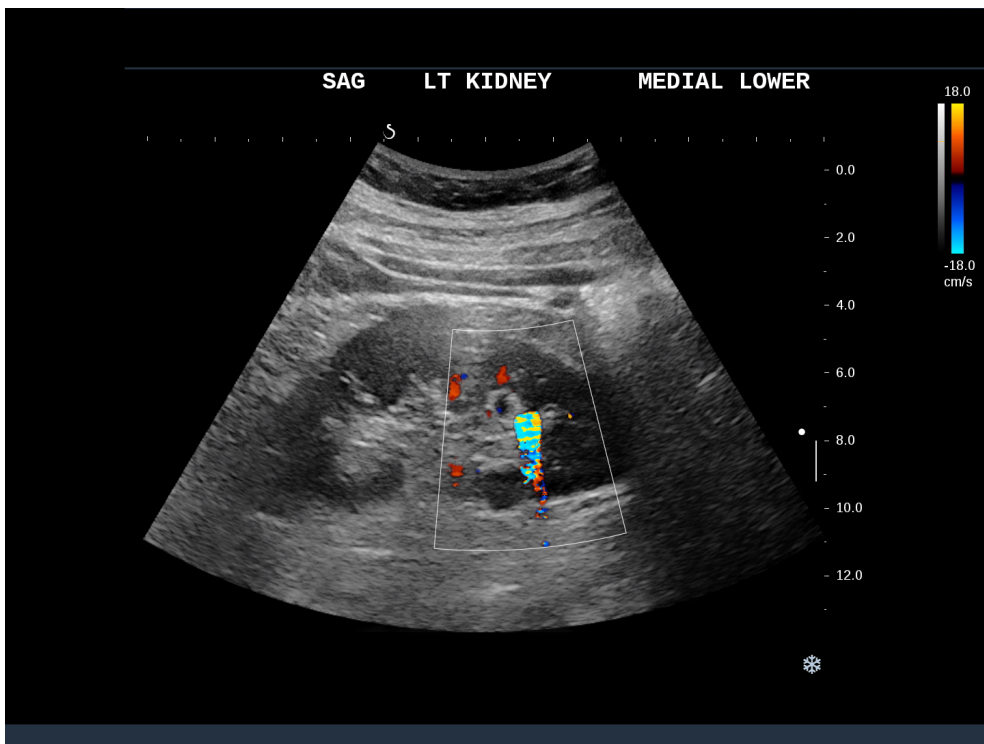


Figure 31 Twinkle Artifact. In this renal ultrasound with doppler flow, a small renal calculi causes the appearance of a twinkle artifact, which manifests as a focus of alternating colors behind the reflective stone.

Figure 32

5.8 Medical Renal Disease

Medical renal disease may result in a hyperechoic (as compared to the liver echogenicity), thin parenchyma and diminished kidney size. However, parenchymal thickness and renal size decrease with age.³⁶

6. Ultrasound of the Bladder

6.1 Anatomical Considerations

Transabdominal bladder sonography is a rapid, inexpensive, and reliable tool with a number of applications in urology (**Table 5**). The patient is positioned supine, and the bladder is imaged through the lower abdomen. For most purposes, it is helpful if the bladder is distended. A curvilinear 5 MHz probe typically provides excellent visualization of the entire bladder. A curved-array transducer is preferred for pelvic sonography, because it requires a smaller skin surface for contact and produces a wider field of the view. The bladder is imaged in the axial plane from dome to trigone. When imaging the trigone and base of the bladder, it is often helpful to apply posterior pressure on the probe as it is directed caudally in order to avoid scatter at the level of the pubic symphysis. **Bladder volume calculations are highly accurate.**³⁷ The most common, and easiest, technique is to multiply measurements obtained in three orthogonal planes. Ureteral efflux from distal ureters can be appreciated using color Doppler. This is best accomplished in the sagittal view with the probe turned in order to align with the direction of the intramural ureter.³⁸

Indications for bladder ultrasound are shown in **Table 5**.⁴

Table 5: Indications for Bladder Ultrasound

Measurement of bladder volume
Measurement of post-void residual
Measurement of prostate size and morphology
Assessment of anatomic changes associated with bladder outlet obstruction
Assessment of vesicoureteral reflux or posterior urethral valves with contrast enhanced voiding urosonogram
Assessment of urethral catheter position
Guidance for suprapubic tube placement
Evaluation of clot burden
Hematuria
Bladder tumor
Evaluation for distal ureteral dilation/distal ureteral stones
Foreign body in bladder
Evaluation of ureterocele
Assessment for bladder neck hypermobility
Evaluation of pelvic fluid collections
Imaging of prostate when the rectum is absent or obstructed

6.2 Trabeculation and Diverticula

Trabeculation of the bladder wall may occur in patients with bladder outlet obstruction and is often accompanied by one or more bladder diverticulae, which are outpouchings of bladder mucosa and submucosa through the muscular wall (**Figure 33**). Sonography provides an ideal modality of imaging diverticula, as the neck can be easily identified, and color Doppler can help determine if there is stagnation within the diverticulum.

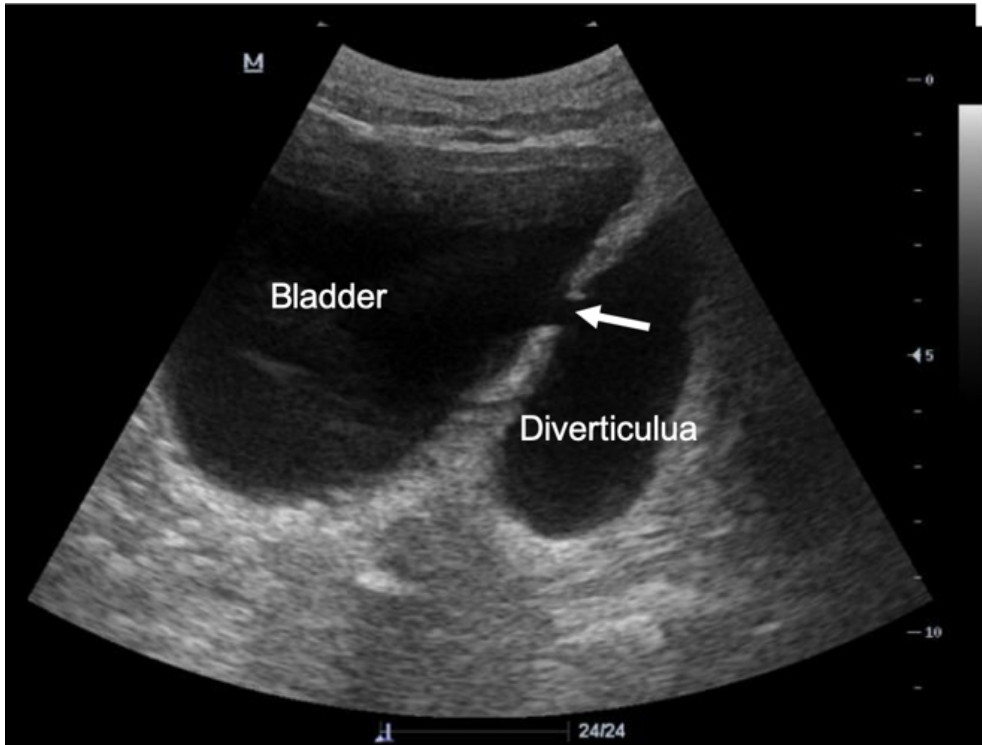


Figure 33:

6.3 Ureteral Dilation

This is a non-specific finding and may result from vesicoureteral reflux, bladder outlet obstruction, tumor, ureteral stricture or distal ureteral stone. In children however, ceVUS is a well-established, sensitive, and safe ultrasound modality for detecting and grading vesicoureteral reflux as well as other lower urinary tract abnormalities.³⁹ Some data suggests that ceVUS is more sensitive than voiding cystourethrogram in the detection of vesicoureteral reflux. **Figure 34** below showcases the ability of ceVUS to detect vesicoureteral reflux.

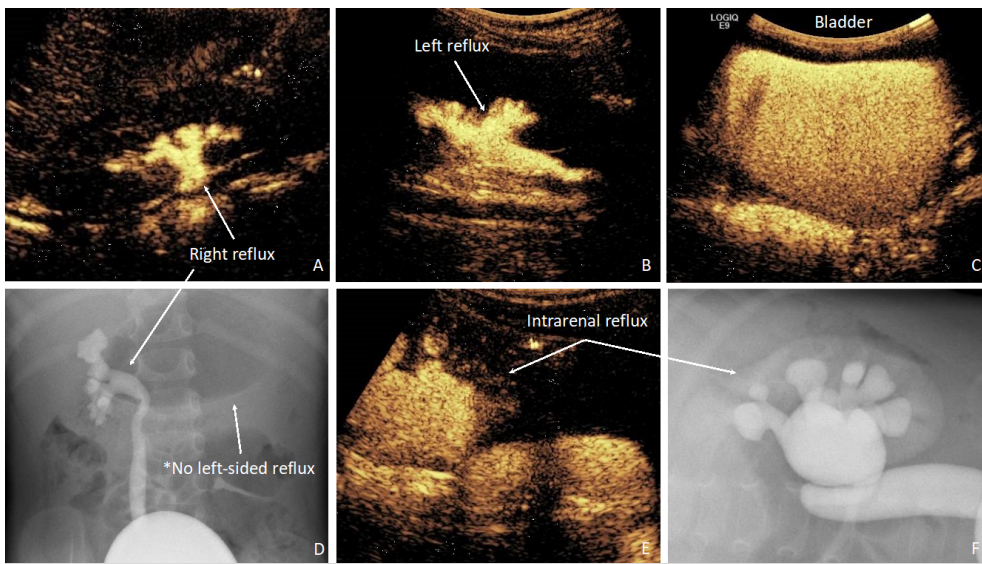


Figure 34: ceVUS for Reflux Evaluation. ceVUS images on a 22-month-old little girl who was being evaluated after recurrent febrile urinary tract infections (A-D). The ceVUS reveals bilateral vesicoureteric reflux (A = reflux on the right and B = reflux on the left) reaching the pelvicalyceal systems. The bladder is filled via a catheter, as seen in image C, and the child voids in the same manner as for conventional fluoroscopic voiding cystourethrography, without the need for ionizing radiation. In this child, a companion voiding cystourethrogram (D), performed on the same day, revealed only right-sided vesicoureteric reflux. In another example, this 8-month-old little girl was evaluated with ceVUS after the fetal observation of urinary tract dilatation and a single febrile UTI (E and F). A magnified view of the inferior aspect of the left kidney reveals a high grade of reflux, with the additional finding of intrarenal reflux. A companion voiding cystourethrogram, oriented in a similar fashion as the ceVUS image, shows the same findings. Images are courtesy of Dr. Carol Barnewolt, pediatric uroradiologist at Boston Children's Hospital.

6.4 Ureteroceles

This refers to the ballooning of the distal ureter. When it is mostly within the submucosa, and only partially projects into the lumen of the bladder, it is termed ectopic (**Figure 35**). When it projects entirely into the bladder, it is considered intravesical or orthotopic.

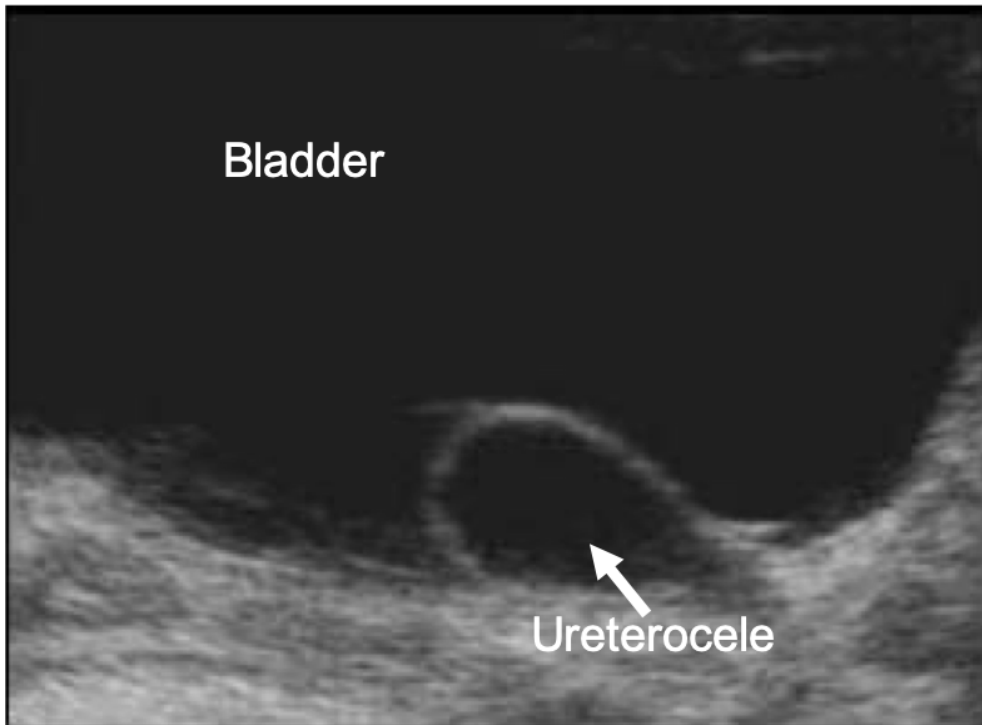


Figure 33 Ureterocele. On this bladder ultrasound, a ureterocele is visualized as a thin wall structure projecting into the lumen of the bladder.

Figure 35

6.5 Bladder Stones

Bladder stone are readily identified on ultrasound as well-defined, mobile echogenic structures with intense acoustic shadowing ([Figure 36](#)).

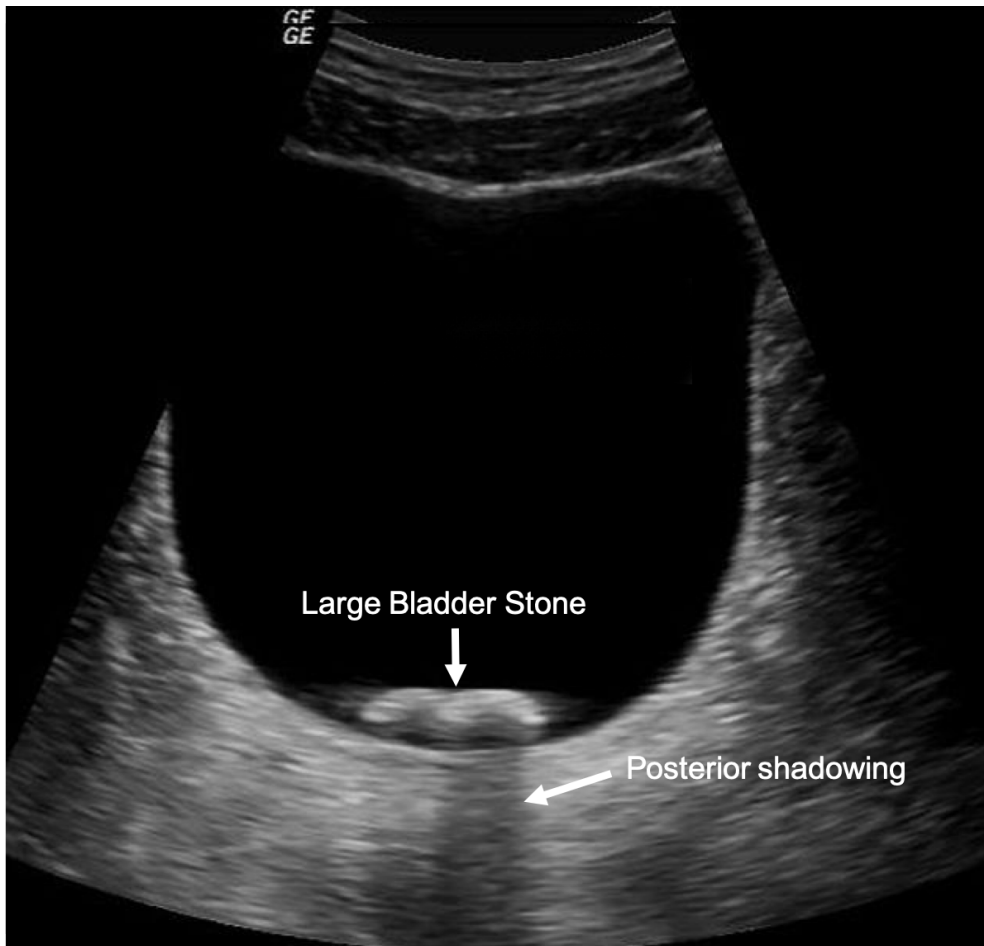


Figure 34 Bladder Stone. On this bladder ultrasound, a large bladder stone is visualized along with a posterior shadowing artifact.

Figure 36

6.6 Neoplasms

While some intravesical tumors can be identified sonographically, the sensitivity of this modality is limited compared to cystoscopy, particularly when the tumor is small (< 5 mm) or located anteriorly ([Figure 37](#)). Depth of invasion cannot be reliably determined.⁴⁰

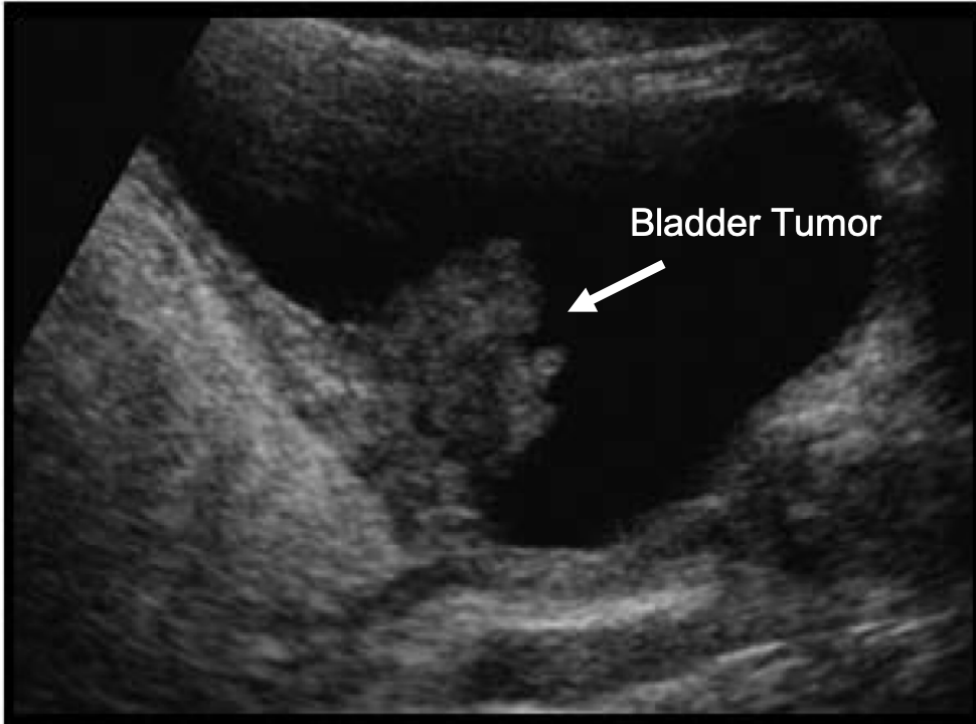


Figure 35 Bladder Tumor. On this bladder ultrasound, a large bladder tumor is visualized as a mass projecting into the bladder lumen.

Figure 37

7. Ultrasonography of the Adrenal Gland

7.1 Anatomical Considerations

The adrenal glands are small, paired organs located anteromedial to the upper pole of the kidneys. The right gland is triangular in shape and lies posterior to the inferior vena cava (IVC), while the left gland is semilunar in shape and lies anteromedial to the upper pole of the left kidney. The normal adrenal glands are thin: 3-6 mm in thickness, 4-6 cm in length and 2-3 cm in width. The right gland is lateral to the crus of the diaphragm, medial to the right lobe of the liver, and posterior to the IVC (usually, the anteromedial ridge of the right gland is located immediately behind the IVC). The left gland is also lateral to the crus of diaphragm and lateral or slightly posterior to the aorta.

Due to the small size of the adrenal glands, **extracorporeal sonography of the normal adrenal gland is challenging**. In contrast, laparoscopic sonography facilitates excellent visualization of the glands, **especially to identify surgical planes**.⁴¹

Adrenal glands in adults are **not** normally visualized on transabdominal ultrasound, especially in obese patients. Any prominent adrenal gland seen on ultrasound should be considered abnormal and further imaging with CT or MRI should be considered. Intra-operative sonography of the adrenal gland is useful during adrenalectomies, particularly in the following cases: small nodules, right-sided adrenal tumors, obese patients, or during partial adrenalectomy.

During **transabdominal sonography**, a curved-array 2.5-6 MHz transducer offers a wide, deep field of the view that is necessary to image the adrenal glands deep in the abdomen. For **laparoscopic**

intra-operative ultrasonography, a linear side-viewing or a flexible side-viewing (preferred) transducer 7.5-10 MHz probe provides excellent ultrasonographic visualization.

Visualization can be compromised as a result of respiratory motion. A single linear scan on sustained deep inspiration can be performed for anterior longitudinal imaging since the inferior vena cava usually distends during deep inspiration, improving sound transmission. The downward motion of the kidney also helps to separate the adrenal gland from the kidney during deep inspiration. Transabdominal subcostal or intercostal views both provide adequate visualization of the adrenal glands. The lateral decubitus position may improve visualization when overlying bowel gas is present. After visualizing the upper pole of the kidney, the probe is directed medially to identify the adrenal gland.

During laparoscopic sonography, the transducer is placed through a standard 10mm port. Typically, the most medial or lateral port is used for the transducer. Rarely, an additional trocar is needed to evaluate the surgical margins of a benign adrenal mass that may be considered for laparoscopic partial adrenalectomy. The upper pole of the kidney should be scanned from medial to lateral in the longitudinal plane until the adrenal gland is identified. If surgical margins are not grossly evident, sonography can be used to determine relationships with other adjacent structures. Doppler ultrasound can also be used to identify vascular structures.

Adrenal masses or hyperplasia may be found incidentally during ultrasound for other indications, but transabdominal ultrasound to specifically assess the adrenal glands may be useful in following patients with an adrenal mass that has not been treated surgically. Additionally, laparoscopic ultrasound is a valuable adjunct to laparoscopic adrenalectomy, facilitating tumor localization and identification of adjacent structures. This technique is particularly helpful for partial adrenalectomies.^{42,43,44,45,46,47}

7.2 Adenomas

Adrenal adenomas are often found incidentally and in most cases are non-functioning. Sonographically, adrenal adenomas appear as well-demarcated, solid nodules, attached to the adrenal limb. Adrenal adenomas are usually isoechoic to the adrenal gland and are hypoechoic relative to the perinephric fat. A left adrenal adenoma can be misdiagnosed as an accessory spleen if its relationship with the adrenal limb is indeterminate.⁴⁸

7.3 Myelolipomas

Adrenal myelolipomas are rare, nonfunctioning tumors composed of varying proportions of bone marrow elements and fat. They arise from the zona fasciculata of the cortex and appear sonographically as echogenic masses. Lesions can be heterogeneous as a result of internal hemorrhage, and if they are predominantly composed of myeloid (as opposed to fat), they can appear iso- or hypo-echoic.

7.4 Pheochromocytoma

Pheochromocytomas are typically large and well-defined on ultrasound, but can appear as homogenous solid structures or can be more heterogenous (**Figure 38**). Bleeding may occur in the medulla, and typically appears as a round to oval echogenic mass in the central part of the gland.⁴⁹



Figure 36 Pheochromocytoma. A pheochromocytoma is visualized as a heterogeneous mass adjacent to the liver.

Figure 38

7.5 Primary Adrenal Carcinomas

Adrenal cortical carcinomas are rare, and the sonographic appearance is variable, depending in part on the size of the lesion. Smaller lesions are homogeneous and appear sonographically similar to adenomas. The mass may have a thin, capsule-like echogenic rim and some calcifications. Larger lesions may contain necrotic material and hemorrhage and can mimic a pheochromocytoma. In some cases, ultrasound can be more informative than CT or MRI. For example, when a large adrenal mass abuts the liver and the origin of the mass is uncertain, anterior displacement of the retroperitoneal fat reflection is strongly suggestive of adrenal origin.⁴⁸

7.6 Lymphoma

Primary adrenal lymphoma is rare, but secondary involvement of the adrenal glands is present in as many as 25% of lymphoma patients. Nearly half of all adrenal lymphomas are bilateral, and the most common type of lymphoma to involve the adrenal gland is non-Hodgkin's lymphoma.

Sonographically, these tumors are echo-poor. However, echogenic areas of necrosis or hemorrhage may be present.

7.7 Metastasis

The adrenal glands are a common site of metastatic disease. Metastatic lesions < 3 cm in size may

appear as a solid homogenous mass, indistinguishable from an adenoma. Larger lesions may demonstrate heterogeneity due to central necrosis or hemorrhage.

Videos

AUA Core Curriculum: Ultrasound

Presentations

Ultrasound Presentation 1

References

- 1 Kossoff G. Basic physics and imaging characteristics of ultrasound. *World Journal of Surgery*. 2000;24(2):134-142.
- 2 † Terris MK, Klaassen Z. Office-Based Ultrasound for the Urologist. *Urologic Clinics of North America*. 2013;40(4):637-647.
A thorough and practical guide to ultrasound in modern Urologic practice.
- 3 Baltaci S, Yagci C, Aksoy H, Elan AH, et al. Determination of transition zone volume by transrectal ultrasound in patients with clinically benign prostatic hyperplasia: agreement with enucleated prostate adenoma weight. *J Urol*. 2000 Jul;164(1):72–5.
- 4 Gilbert B. Urologic Ultrasound Protocols, In *Practical Urological Ultrasound Second Edition*, Fulgham PF and Gilbert BR editors, Humana Press, 292-344, 2017.
- 5 ☆ Lerner LB, McVary, KT, Barry MJ et al: Management of lower urinary tract symptoms attributed to benign prostatic hyperplasia: AUA Guideline part II, surgical evaluation and treatment . *J Urol* 2021; 206: 818.
- 6 ☆ Onur R, Littrup PJ, Pontes JE, BIANCO JR FJ. Contemporary impact of transrectal ultrasound lesions for prostate cancer detection. *The Journal of Urology*. 2004;172(2):512-514.
- 7 † Trabulsi EJ HE, Gomella LG. Ultrasonography and biopsy of the prostate Vol 102011.
Well written and thorough review of fundamental urologic diagnostic techniques.
- 8 Boehm K et al, Shear Wave Elastography for Localization of Prostate Cancer Lesions and Assessment of Elasticity Thresholds: Implications for Targeted Biopsies and Active Surveillance Protocols, *J Urol*, 193(3),794-800, 2015

- 9 ☆ Lightner DJ, Wymer K, Sanchez J et al: Best practice statement on urologic procedures
and antimicrobial prophylaxis. *J Urol* 2020; 203: 351.
- 10 Berger AP, Frauscher F, Halpern EJ, et al. Periprostatic administration of local anesthesia
during transrectal ultrasound-guided biopsy of the prostate: a randomized, double-blind,
placebo-controlled study. *Urology*. 2003;61(3):585-588.
- 11 Trucchi A, De Nunzio C, Mariani S, Palleschi G, Miano L, Tubaro A. Local anesthesia reduces
pain associated with transrectal prostatic biopsy. *Urologia internationalis*. 2005;74(3):209-213.
- 12 ☆ Lee HY, Lee HJ, Byun S-S, Lee SE, Hong SK, Kim SH. Effect of intraprostatic local
anesthesia during transrectal ultrasound guided prostate biopsy: comparison of 3 methods in a
randomized, double-blind, placebo controlled trial. *The Journal of Urology*.
2007;178(2):469-472.
- 13 ☆ Cam K, Sener M, Kayikci A, Akman Y, Erol A. Combined periprostatic and intraprostatic
local anesthesia for prostate biopsy: a double-blind, placebo controlled, randomized trial. *The
Journal of Urology*. 2008;180(1):141-145.
- 14 Mai Z, Yan W, Zhou Y, et al. Transperineal template-guided prostate biopsy: 10 years of
experience. *BJU Int*. 2016;117:424–429. DOI: 10.1111/bju.13024
- 15 Meyer AR, Joice GA, Schwen ZR, et al. Initial Experience Performing In-office
Ultrasound-guided Transperineal Prostate Biopsy Under Local Anesthesia Using the
PrecisionPoint Transperineal Access System. *Urology* 2018;115:8-13 DOI:
10.1016/j.urology.2018.01.021,
- 16 Tomova A, Deepinder F, Robeva R, Lalabonova H, Kumanov P, Agarwal A. Growth and
development of male external genitalia: a cross-sectional study of 6200 males aged 0 to 19
years. *Archives of Pediatrics & Adolescent Medicine*. 2010;164(12):1152-1157.
- 17 Paltiel HJ, Diamond DA, Di Canzio J, Zurakowski D, Borer JG, Atala A. Testicular volume:
comparison of orchidometer and US measurements in dogs. *Radiology*. 2002 Jan;222(1):114-9.
doi: 10.1148/radiol.2221001385. PMID: 11756714.
- 18 Micallef M, Ahmad I, Ramesh N, Hurley M, McInerney D. Ultrasound features of blunt testicular
injury. *Injury*. 2001;32(1):23-26.
- 19 Liang T, Metcalfe P, Sevcik W, Noga M. Retrospective review of diagnosis and treatment in
children presenting to the pediatric department with acute scrotum. *AJR Am J Roentgenol*.
2013;200(5):W444–W449
- 20 Bertolotto M. Color Doppler US of the penis. Springer; 2008.

- 21 Levine L, Rybak J, Corder C, Farrel MR. Peyronie's Disease Plaque Calcification-Prevalence, Time to Identification, and Development of a New Grading Classification. *The Journal of Sexual Medicine*. 2013;10(12):3121-3128.
- 22 ☆ † Morey AF, McAninch J. Sonographic staging of anterior urethral strictures. *The Journal of Urology*. 2000;163(4):1070-1075.
A seminal paper in urethral imaging.
- 23 Barnewolt, C. E., Acharya, P. T., Aguirre Pascual, E., Back, S. J., Beltrán Salazar, V. P., Chan, P., Chow, J. S., Coca Robinot, D., Darge, K., Duran, C., Klju?evšek, D., Kwon, J. K., Ntoulia, A., Papadopoulou, F., Wo?niak, M. M., & Piskunowicz, M. (2021). Contrast-enhanced voiding urosonography part 2: urethral imaging. *Pediatric radiology*, 10.1007/s00247-021-05116-6. Advance online publication. <https://doi.org/10.1007/s00247-021-05116-6>
- 24 Feldman, H. A., Johannes, C. B., Derby, C. A. et al.: Erectile dysfunction and coronary risk factors: prospective results from the Massachusetts male aging study. *Prev Med*, 30: 328, 2000
- 25 Blumentals, W. A., Gomez-Caminero, A., Joo, S. et al.: Should erectile dysfunction be considered as a marker for acute myocardial infarction? Results from a retrospective cohort study. *Int J Impot Res*, 16: 350, 2004
- 26 Sikka SC, Hellstrom WJ, Brock G, Morales AM. Standardization of Vascular Assessment of Erectile Dysfunction. *The Journal of Sexual Medicine*. 2013;10(1):120-129.
- 27 ☆ Rahman, N.U., et al., Crural ligation for primary erectile dysfunction: a case series. *J Urol*, 2005. 173(6): p. 2064-6.
- 28 ☆ Qureshi JM, Wood H, Feldman M. High Flow Priapism on Color Doppler Ultrasound. *The Journal of Urology*. 2013;189(6):2312-2313.
- 29 Datta S, Allen G, Evans R, Vaughton K, Lucas M. Urinary tract ultrasonography in the evaluation of haematuria--a report of over 1,000 cases. *Annals of the Royal College of Surgeons of England*. 2002;84(3):203.
- 30 Nguyen HT, Benson CB, Bromley B, Campbell JB, Chow J, Coleman B, et al. Multidisciplinary consensus on the classification of prenatal and postnatal urinary tract dilation (UTD classification system). *J Pediatr Urol*. 2014;10:982
- 31 Medicine AloUi. Ultrasound in the practice of urology. 2011;
- 32 Chi T, Usawachintachit M, Mongan J, et al. Feasibility of Antegrade Contrast-enhanced US Nephrostograms to Evaluate Ureteral Patency. *Radiology*. 2017; 283(1): 273–279.

- 33 Bosniak MA. The current radiological approach to renal cysts. *Radiology*. 1986;158(1):1-10.
- 34 Bukavina, L., Mishra, K., Calaway, A., & Ponsky, L. (2021). Robotic Partial Nephrectomy: Update on Techniques. *The Urologic clinics of North America*, 48(1), 81–90.
<https://doi.org/10.1016/j.ucl.2020.09.013>
- 35 ☆ Passerotti, C., Chow, J. S., Silva, A. et al.: Ultrasound versus computerized tomography for evaluating urolithiasis. *J Urol*, 182: 1829, 2009
- 36 Gourtsoyiannis N, Prassopoulos P, Cavouras D, Pantelidis N. The thickness of the renal parenchyma decreases with age: a CT study of 360 patients. *AJR. American Journal of Roentgenology*. 1990;155(3):541-544.
- 37 Maymon R, Gilboa S, Abramowicz J, Shulman A, Toar M, Bahary C. Ultrasonic validation of residual bladder volume in postvaginal hysterectomy patients. *Gynecologic and Obstetric Investigation*. 1991;31(4):226-230.
- 38 Denis L. Future implications for the management of benign prostatic hyperplasia. *European Urology*. 1993;25:29-34.
- 39 Ntoulia, A., Aguirre Pascual, E., Back, S. J., Bellah, R. D., Beltrán Salazar, V. P., Chan, P., Chow, J. S., Coca Robinot, D., Darge, K., Duran, C., Epelman, M., Klju?evšek, D., Kwon, J. K., Sandhu, P. K., Wo?niak, M. M., & Papadopoulou, F. (2021). Contrast-enhanced voiding urosonography, part 1: vesicoureteral reflux evaluation. *Pediatric radiology*, 10.1007/s00247-020-04906-8. Advance online publication.
<https://doi.org/10.1007/s00247-020-04906-8>
- 40 Ozden E, Turgut AT, Turkolmez K, Resorlu B, Safak M. Effect of bladder carcinoma location on detection rates by ultrasonography and computed tomography. *Urology*. 2007;69(5):889-892.
- 41 Chow G, Blute M. Surgery of the adrenal glands. *Campbell-Walsh Urology*. 2007;9:1868-1888.
- 42 Birnholz JC. Ultrasound Imaging of Adrenal Mass Lesions 1. *Radiology*. 1973;109(1):163-166.
- 43 Forsythe JR, Gosink BB, Leopold GR. Ultrasound in the evaluation of adrenal metastases. *Journal of Clinical Ultrasound*. 1977;5(1):31-34.
- 44 Lockhart ME, Smith JK, Kenney PJ. Imaging of adrenal masses. *European Journal of Radiology*. 2002;41(2):95-112.
- 45 Wilson SR, Withers C, Wilson S, Charboneau W. Diagnostic ultrasound. Philadelphia: Elsevier Mosby Publisher. 2005;853:863.

- 46 ☆ Pautler SE, Choyke PL, Pavlovich CP, Daryanani K, Walther MM. Intraoperative ultrasound aids in dissection during laparoscopic partial adrenalectomy. *The Journal of Urology*. 2002;168(4):1352-1355.
- 47 Kim FJ, Rove K, Sehrt DE. Intraoperative Urologic Ultrasound. *Practical Urological Ultrasound*: Springer; 2013:223-241.
- 48 Fan J, Tang J, Fang J, et al. Ultrasound Imaging in the Diagnosis of Benign and Suspicious Adrenal Lesions. *Medical Science Monitor: International Medical Journal of Experimental and Clinical Research*. 2014;20:2132.
- 49 Raja A, Leung K, Stamm M, Grgis S, Low G. Multimodality imaging findings of pheochromocytoma with associated clinical and biochemical features in 53 patients with histologically confirmed tumors. *American Journal of Roentgenology*. 2013;201(4):825-833.